To the Graduate Council:

I am submitting herewith a thesis written by Dennis Ray Knisley entitled "Reaction Kinetics of the Downstream MHD Process Gas Before Secondary Combustion." I have examined the final copy of this thesis for form and content and recommend that it be accepted in partial fulfillment of the requirements for the degree of Master of Science, with a major in Chemical Engineering.

Lloyd W. Crawford, Major Professor

We have read this thesis
and recommend its acceptance:

R. M. Conway

Arnold C. Smith

Accepted for the Council:

Vice Provost
and Dean of The Graduate School

STATEMENT OF PERMISSION TO USE

In presenting this thesis in partial fulfillment of the requirements for a Master's degree at The University of Tennessee, Knoxville, I agree that the Library shall make it available to borrowers under rules of the Library. Brief quotations from this thesis are allowable without special permission, provided that accurate acknowledgment of source is made.

Permission of extensive quotation from or reproduction of this thesis may be granted by my major professor, or in his absence, by the Head of Interlibrary Services when, in the opinion of either, the proposed use of the material is for scholarly purposes. Any copying or use of the material in this thesis for financial gain shall not be allowed without my written permission.

Signature Dennis R. Knisley

Date 11/21/85

REACTION KINETICS OF THE DOWNSTREAM MHD PROCESS GAS BEFORE SECONDARY COMBUSTION

A Thesis

Presented For the

Master of Science

Degree

The University of Tennessee, Knoxville

Dennis Ray Knisley

December 1985

DEDICATION

To my father, the late Benjamin H. Knisley, Jr.

ACKNOWLEDGMENTS

The work presented herein was accomplished with great support received from my colleagues at The University of Tennessee Space Institute. Initially, I would like to thank my major professor, Dr. Lloyd Crawford, for his help in establishing the theoretical model used herein, and to my committee, Drs. Atul Sheth and Robert Counce for reviewing this text. The experimental work was accomplished with much support from my work supervisor, Mr. Patrick Lynch, in addition to Mr. Alan Tate, Mr. William Baucum and Mr. Robert Douglas. Finally, my thanks to the Chemical Laboratory personnel, Mr. Phil Sherrill and Mrs. Kathy Hines, and to Dr. Fred L. Galanga for the use of his heat transfer code.

All work presented was sponsored by the United States Department of Energy under Contract No. DEA-AC02-79ET10815.

ABSTRACT

The reaction kinetics of the MHD downstream process gas before secondary combustion are examined here. Emphasis is placed on the decomposition of nitrogen oxide into ammonia fractions and hydrogen cyanide but sulfur and carbon containing species reactions are also considered. The shift in species concentrations at the refractory furnace and secondary combustor inlet gas sample probes are modeled using the "Premixed One-Dimensional Flame" (PROF) code. In addition, a heat transfer analysis of the sample probe is involved. This was evaluated so that a more accurate analysis of the actual combustion gas in the flow train could be established from the experimental data collected during the test runs. The results gathered from this code were analyzed with experimental data collected during the LMF3B test series. The PROF code modeled the nitrogen species reactions with reasonable accuracy while some discrepancy was seen between the theoretical and experimental results involving the sulfur and carbon species.

TABLE OF CONTENTS

LIST OF TABLES

LIST OF FIGURES

FIGURE PAGE

NOMENCLATURE

A	cross sectional area of the bounding tube
C_j	input parameter used to run PROF
C_{p_i}	specific heat of species i
C_W	circumference of bounding tube
D	diameter of bounding tube
g	Gibbs free energy of bulk gas
h	enthalpy of bulk gas
$\bar{h}$	average convective heat transfer coefficient
H_i	enthalpy of pure species i
J_{W_i}	flux of species i at bounding tube wall
k	thermal conductivity
$\dot{m}$	mass flow rate
n	total number of moles
n_i	number of moles of species i
Nu_D	Nusselt number for internal flow
p	perimeter
P	pressure
q	axial heat flux
q_w	heat transport at the bounding tube wall
Q	volumetric heat loss
R	universal gas constant
Re_D	Reynolds number for internal flow
S	distance along axis
t	time

T	temperature
V	specific volume
W_i	chemical production rate of species i
x	axial distance
Y_i	mass fraction of species i
ρ	density
μ	dynamic viscosity
μ_i	chemical potential of species i
μ_i^0	chemical potential of species i in the standard state

Subscripts

g	gaseous
i	ith species
W	inner wall of tube

Superscripts

0	standard state

1.0 INTRODUCTION

A coal-fired magnetohydrodynamic (MHD) combined cycle power plant differs from a conventional coal-fired power plant in several important aspects. Two of these, the higher combustion temperature and pressure required by the MHD topping cycle, lead to the formation of very high levels of nitrogen oxides (NO_x)[1]. At The University of Tennessee Space Institute (UTSI) Coal Fired Flow Facility (CFFF) secondary combustion is used to control the NO_x levels within the Environmental Protection Agency (EPA) limits. In addition, the cooling through the radiant furnace enhances the decomposition of NO_x via ammonia fragments and sulfur chemical reactions [1]. In order to evaluate the levels of NO_x and other constituents in the MHD downstream gas (CO, CO_2, O_2, and SO_2), there are six gas sampling probes located along the flow train. A schematic diagram of the CFFF showing the sample probe locations is shown in Figure 1.

The samples analyzed are extracted from the flow train through stainless steel, water cooled sample probes using an air eductor. A portion of this gas is extracted, then filtered and dried before it reaches the detection devices. This paper will address the shift in species concentrations which occur through the sample probes at the sample locations prior to the secondary combustor. The chemical kinetics will be modeled using the "Premixed One-Dimensional Flame" (PROF) computer code. The plug-flow option with convective heat transfer coefficient input was used in this analysis. This required analysis of the heat transfer through the sample probe to determine an average

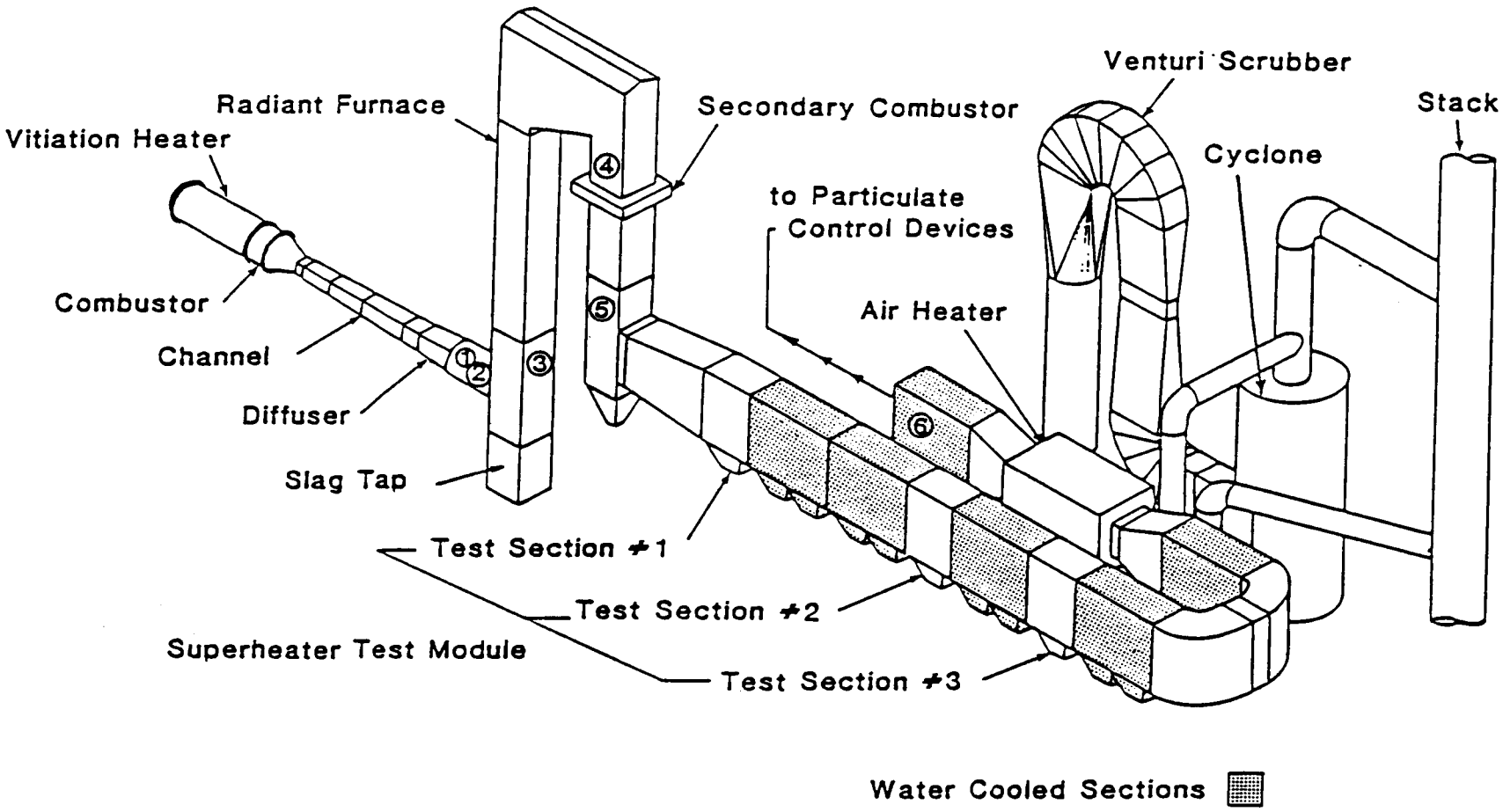

Figure 1. Schematic Diagram of CFFF Flow Train for the LMF3B Test Series.

heat transfer coefficient. Other inputs necessary to run the PROF code include the initial gas composition at the sample probe entrance; the initial gas temperature; pressure; flow rate of the gas; the probe wall temperature; and a reaction set. The PROF code was used to conduct a chemical kinetic analysis of reactions, especially of nitrogen oxides, but also of other nitrogen and sulfur species through the sample probes at the radiant furnace (RF1) and the secondary combustor inlet (SCI).

Experimental results collected during the LMF3B test series were analyzed with respect to the theoretical results obtained using the PROF code. The LMF3B test series consisted of three tests run between late September and mid-November during 1984. A test consists of preheating the CFFF flow train with auxiliary burners and the vitiation heater burning fuel oil. When preheating is complete, the system is converted to coal combustion through the primary combustor. The primary stoichiometry for the LMF3B test series was 0.85 when running on coal. The initial test, LMF3B-1, was run on September 27. The test consisted of approximately seven hours on coal between 8:00 A.M. and 3:00 P.M. The second test, LMF3B-2a, was run on October 25 and consisted of approximately three hours on coal between 7:30 A.M. and 10:30 A.M. The final test, LMF3B-2b, was run on November 15, and consisted of approximately eight hours on coal between 7:00 A.M. and 3:00 P.M. During the first and third tests, data was collected for the heat transfer analysis of the probe at the RF1 sample location. During all three tests the levels of nitrogen oxide (NO) and carbon monoxide in the gas stream were monitored continuously at the RF1 and

SCI sample locations. In addition to these constituents, the levels of hydrogen sulfide (H_2S), ammonia (NH_3), and hydrogen cyanide (HCN) in the dry gas sample were monitored at selected times during the tests. Finally, during test LMF3B-2b the on line gas chromatograph which analyzes for CO, nitrogen (N_2), oxygen (O_2), carbon dioxide (CO_2), methane (CH_4), and hydrogen (H_2) was used at the SCI sample location. A gas sampling log can be found in Appendix A. These experimental results were compared with the theoretical results obtained with the PROF code to establish a better analysis of the combustion gas in the CFFF flow train.

2.0 THEORETICAL ANALYSES

2.1 Theoretical Modeling of the Chemical Kinetics

The "Premixed One-dimensional Flame" (PROF) code was used to model the chemical kinetics of the MHD downstream gas. The PROF code can numerically model the detailed chemical kinetics of premixed flame, well-stirred reactor, plug-flow reactor, and fixed mass time-evolution problems. The plug-flow reactor option with nonreactive wall was used in this case to model the chemical kinetics through the gas sample probes at the radiant furnace entrance and the secondary combustor inlet. Radial convective heat transfer was considered by the plug-flow reactor option. The governing conservation equations for this option are [2]:

$$\underline{\text{Species}} \qquad \dot{m}\frac{dY_i}{ds} = AW_i - C_W J_{W_i} \tag{1}$$

$$\underline{\text{Energy}} \qquad \dot{m}\frac{dh}{ds} = AQ - C_W q_W \tag{2}$$

The boundary conditions necessary to solve these equations were the initial gas composition and temperature values.

The inputs needed to run PROF included the initial concentrations of the reacting species, pressure, initial temperature, and a reaction set. The special input needed for the plug-flow reactor option was the convective heat transfer coefficient and the reactor wall temperature. The determination of these inputs will be discussed in

subsequent sections. The output for the code includes time, enthalpy, temperature, density, system molecular weight, and individual species concentrations at each specified grid point along the reactor.

2.2 Determination of Initial Gas Composition at the Sample Probe Entrance

Calculation of the initial concentrations of the MHD downstream gas at the sample probes was accomplished using the PROF code and the NASA-SP273 Equilibrium (NASA) code. The NASA code is a computer program capable of calculating chemical equilibrium compositions for assigned thermodynamic states; determining theoretical rocket performance; doing Chapman-Jouguet detonations; and doing shock tube parameter calculations. This program considers all gases to be ideal mixtures and is capable of dealing with pure condensed species. The equation of state used by the code is then [3]:

$$\frac{P}{\rho} = PV = nRT \tag{3}$$

This equation is assumed to be correct even in the presence of a small amount of condensed species; in which case, it is assumed that the condensed species occupy negligible volume and exert negligible pressure compared to the gaseous species.

Chemical equilibrium can be denoted by two methods, equilibrium constants or minimization of free energy. The NASA code utilizes minimization of the Gibbs or Helmholtz free energy as the condition for equilibrium. For use in this case the thermodynamic state was specified by setting the temperature and pressure, in which case the

NASA code uses the minimization of the Gibbs free energy. The Gibbs free energy per kilogram of mixture is given by [3]:

$$g = \sum_{i=1}^{n} \mu_i n_i \tag{4}$$

where the chemical potential is given by:

$$\underline{\text{gases}} \qquad \mu_i = \mu_i^0 + RT\ln\frac{n_i}{n} + RT\ln P \tag{5}$$

$$\underline{\text{condensed species}} \quad \mu_i = \mu_i^0 \tag{6}$$

The NASA code uses a Newton-Raphson method to find the minimum Gibbs free energy at the assigned temperatures and pressures and hence the composition and thermodynamic properties at chemical equilibrium.

The NASA code was used to determine the composition of the combustion gas at the diffuser exit for tests LMF3B-1, LMF3B-2a, and LMF3B-2b. The gas is assumed to be in equilibrium at this point because of the high temperatures and residence time in the diffuser. The temperature at this point is 2400K and the pressure is approximately 1 atm. The other inputs necessary to run the NASA code were the flow rates of the oxyen, nitrogen, coal, and potassium carbonate seed for the specific times of interest, which were obtained from the test reports. The NASA output was used as the initial concentrations for the PROF code to develop a gas composition profile through the CFFF flow train from the diffuser exit to the secondary combustor.

In order to obtain the composition profile for the MHD downstream gas the time-evolution option for the PROF code was used. This option is capable of handling the reactions of a fixed mass of gas in time as the pressure and temperature change. The governing conservation equations for this option are [2]:

$$\underline{\text{Species}} \quad dY_i = \frac{dt}{\rho} W_i \tag{7}$$

while the energy equation is the same as Equation (2) for the plug flow option. The boundary conditions needed to solve these equations are the initial mixture composition, which was obtained from NASA, and the assigned pressure and temperature through the flow train. The time-temperature-pressure data required as an input was obtained from Dr. Fred Galanga using a computer code developed for the United States Department of Energy and described in Reference [4]. This program considers the radiation heat transfer between the gas and the downstream components and calculates the thermodynamic state at specified points along the flow train. The code considers that the gas is in chemical equilibrium and calculates local gas velocity and residence time through mass conservation. The output includes the residence time and temperature of the MHD downstream gas at the center of the CFFF flow train at the specified computational stations.

Using the previously determined inputs, the PROF code was run to obtain a composition profile for the 30 species of interest at specified intervals along the CFFF flow train including the radiant furnace

(RF1) and secondary combustor inlet (SCI) sample probes. These output values were used as initial concentrations when PROF was run for the RF1 and SCI gas sample probes. A slight adjustment was made in the NO concentration to be consistent with the NO/NO_x detectors used during the test at the previously mentioned sample locations. The NO concentration was changed to that detected at the time of interest and the N_2 concentration was adjusted to keep the nitrogen balance. The oxygen balance was adjusted by altering the CO and CO_2 concentrations.

2.3 Determination of the Heat Transfer Coefficient Through the Sample Probe

The convective heat transfer coefficient for the gas sample probes was determined at the RF1 sample location. This required analysis of the gas flow through the sample probe. The gas sample is taken from the flow train by a Perma Pure Products Teflon® eductor through a water cooled sample probe. A performance curve for the eductor is shown in Figure 2 which displays the volumetric flow rate versus the pressure across the orifice. During tests the pressure across the orifice is kept between 8 and 12 psia. Using this flow rate and the physical properties of nitrogen at an average gas temperature through the probe of 1300K, the Reynolds number for the gas was determined using:

$$Re_D = \frac{4\dot{m}}{\pi D \mu} \tag{8}$$

The Reynolds numbers at 5, 10, and 15 psia were found to be 47, 50, and 53, respectively. Therefore, an average value of 50, which is in

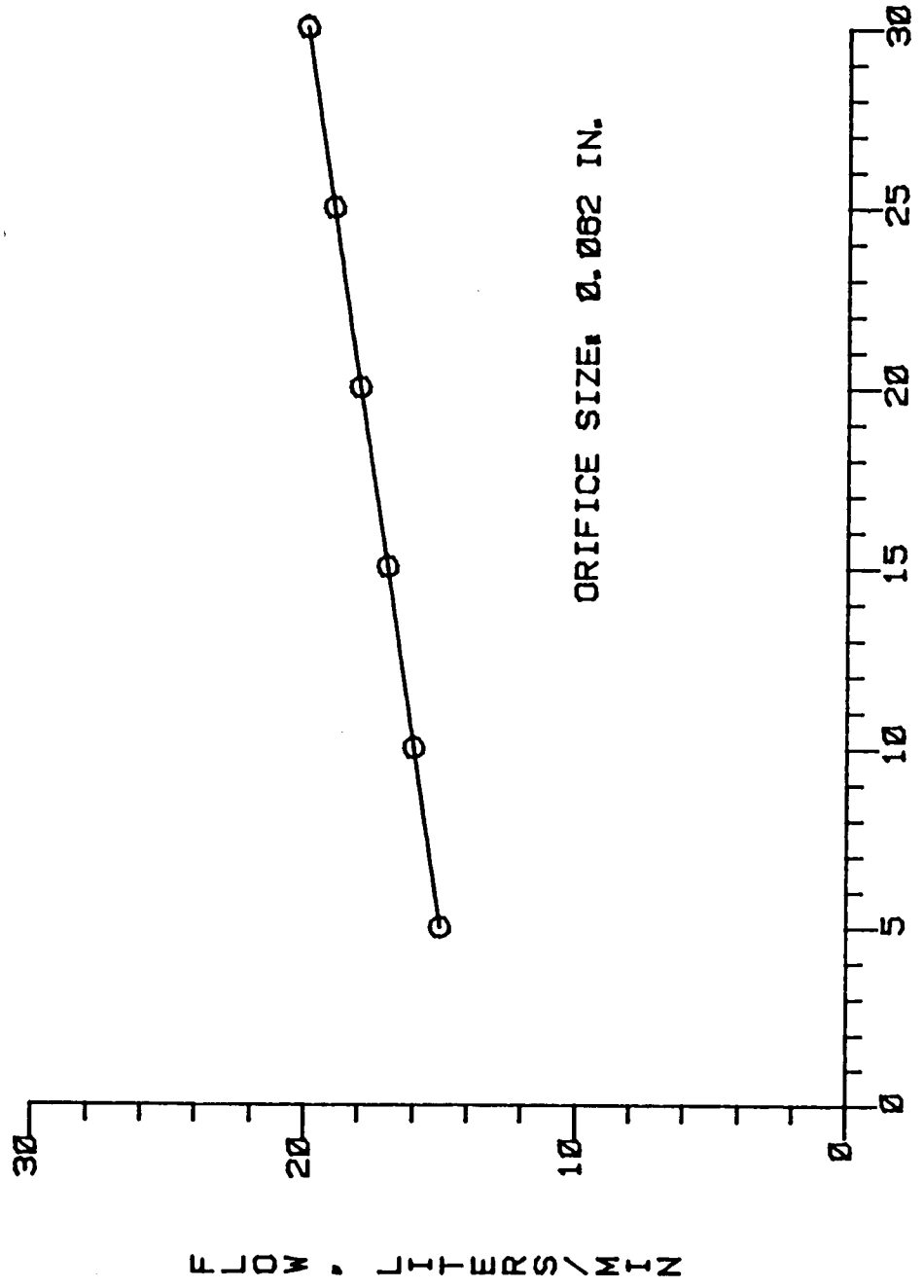

Figure 2. Performance Curve for the Perma Pure Teflon® Eductor Model ED-F.

the low Reynolds number regime, was used in further calculations. It was then determined that the Nusselt number was 3.66 using the correlation for laminar flow in circular tubes with constant surface temperature [5]. Using this Nusselt number the heat transfer coefficient was found by the following equation [5]:

$$\bar{h} = \frac{Nu_D k}{D} \tag{9}$$

Again, the physical properties of nitrogen at 1300K were used and the diameter (D) of the tube was 0.0381 meters. The average convective heat transfer coefficient ($\bar{h}$) for the sample probe was found theoretically to be 7.78 W/m^2K. The PROF code with plug-flow reactor option requires an input of a C_j factor which is defined [2]:

$$C_j = \frac{\bar{h}D/k}{D^2} = \frac{Nu_D}{D^2} \tag{10}$$

Using the average heat transfer coefficient calculated above a theoretical temperature profile through the sample probe was calculated for tests LMF3B-1 and LMF3B-2b.

During tests LMF3B-1 and LMF3B-2b a special sample probe with thirteen thermocouples along the length of the probe was used at the RF1 sample location, shown in Figure 3. Using the data collected from this sample probe an actual gas temperature profile through the sample probe was constructed. Plots of the raw data can be found in Appendix B. This temperature profile, along with the theoretical temperature profile determined with the PROF code, is shown in Figure 4 for test LMF3B-1 and Figure 5 for test LMF3B-2b. It was apparent from these plots that the theoretical heat transfer coefficient was not high

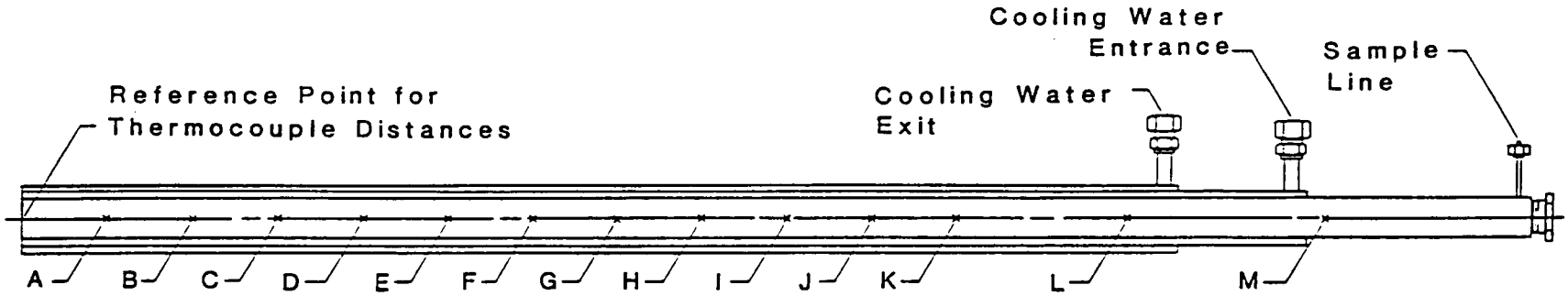

NOTE:

Thermocouple	Distance (m)	Thermocouple	Distance (m)
A	0.076	H	0.609
B	0.152	I	0.685
C	0.228	J	0.762
D	0.304	K	0.838
E	0.381	L	0.990
F	0.457	M	1.168
G	0.533		

Total Probe Length = 1.354 m

Figure 3. Water Cooled Sample Probe Equipped with Thermocouples to Determine the Gas Temperature Profile.

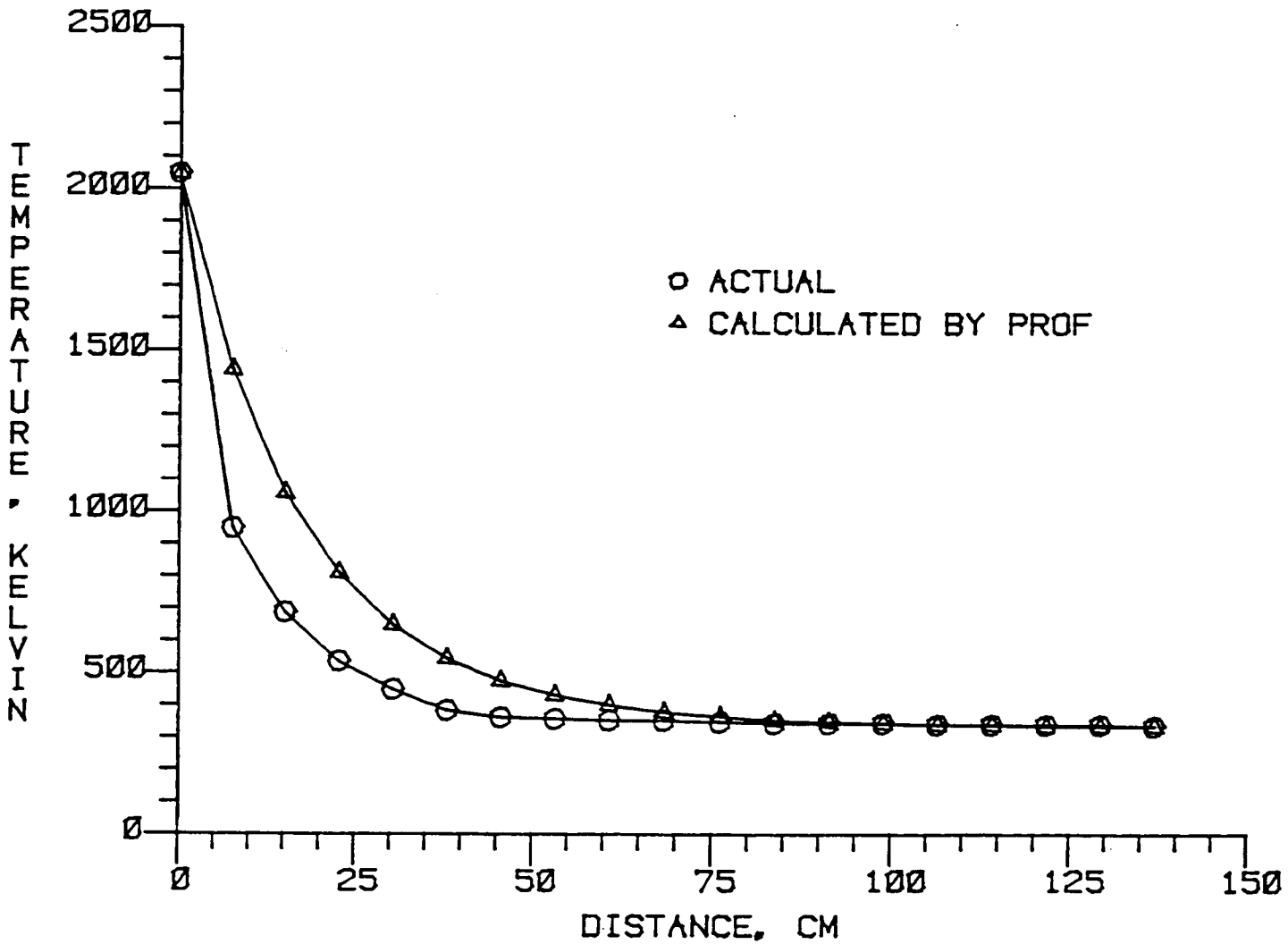

Figure 4. Gas Temperature Profile for Test LMF3B-1 with the Heat Transfer Coefficient Equal to 7.78 W/m^2K.

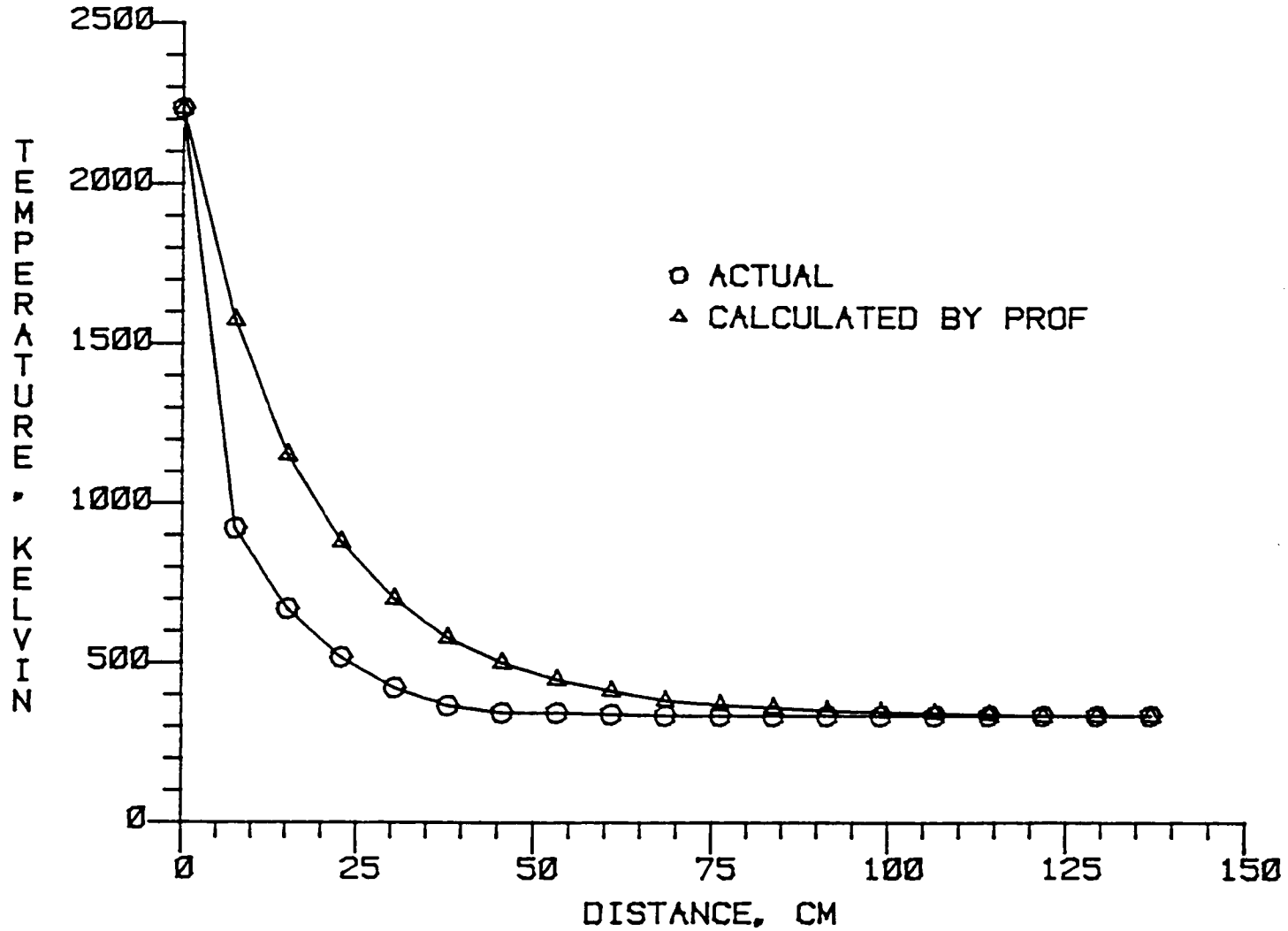

Figure 5. Gas Temperature Profile for Test LMF3B-2b with the Heat Transfer Coefficient Equal to 7.78 W/m^2K.

enough since the actual temperature profile dropped much quicker than the theoretical profile. This could be attributed to the use of a constant surface temperature correlation to determine the Nusselt number when this is not literally the case for the sample probe. Hence, the PROF code was run several more times varying only the heat transfer coefficient. The best fit between the theoretical and actual data was found when the convective heat transfer coefficient was 17.78 W/m^2K. These gas temperature profiles are shown in Figures 6 and 7 for tests LMF3B-1 and LMF3B-2b, respectively. Using this valve for $\bar{h}$ and Equation (9) the Nusselt number for the for the flow through the sample probes was determined to be 8.36.

2.4 Theoretical Thermodynamic Calculations

The PROF code does not include condensed species. Since condensed phase transitions can cause larger enthalpy-temperature variations than observed with gaseous species, a computer code was developed using theoretical heat transfer-enthalpy relations and compared to the PROF and experimental results. For internal flow through a tube the heat transfer between the tube wall and gas can be related to the temperature difference as follows [6]:

$$dq = \bar{h}dA(T_g - T_w) \tag{11}$$

Also, the heat transfer can be related to the change in enthalpy by the following equation [5]:

$$dq = \dot{m}dh \tag{12}$$

By equating the two above equations and using the relationship $dA = p\,dx$ a relationship between the change in enthalpy over distance

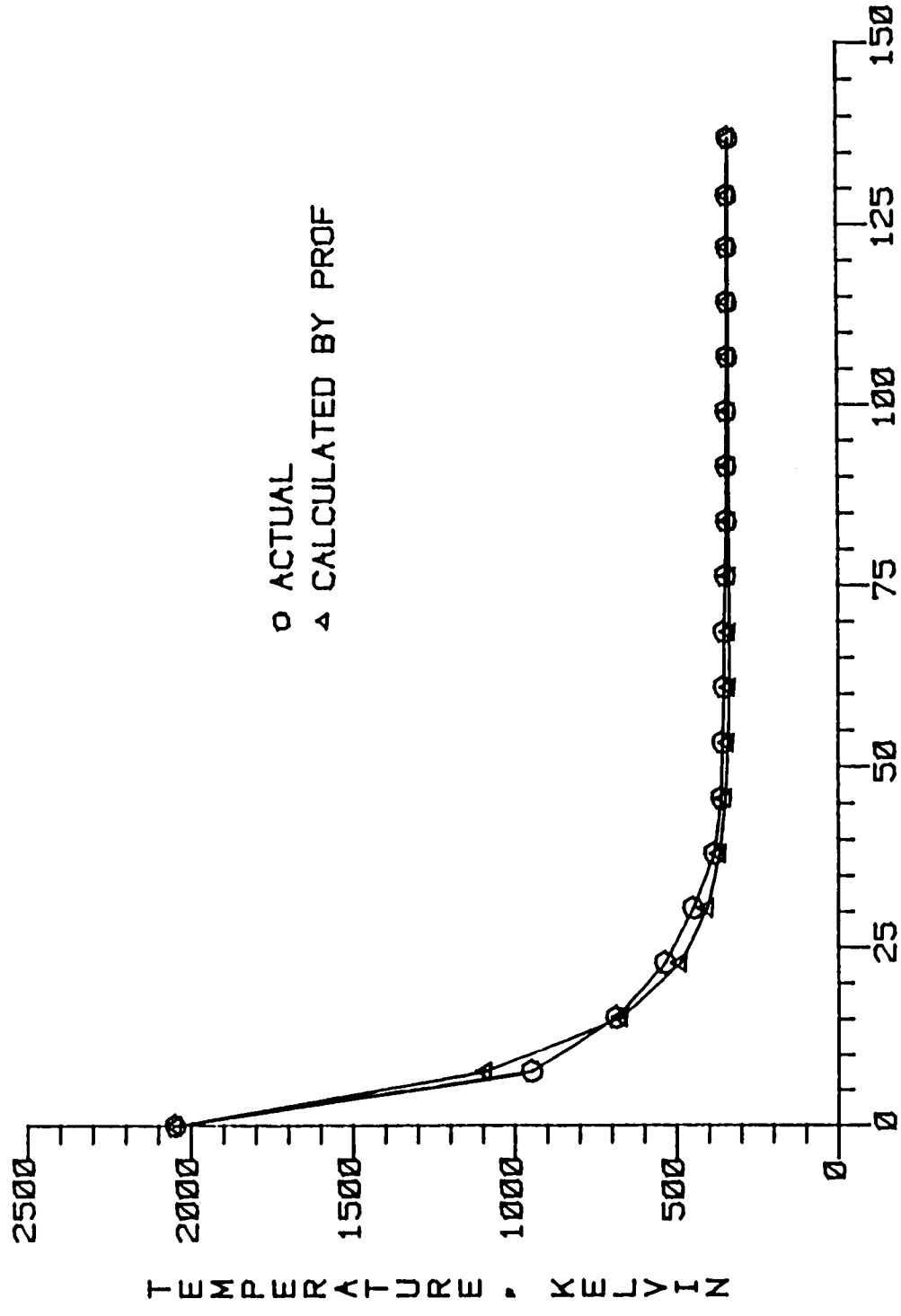

Figure 6. Gas Temperature Profile for Test LMF3B-1 with the Heat Transfer Coefficient Equal to 17.78 W/m^2K.

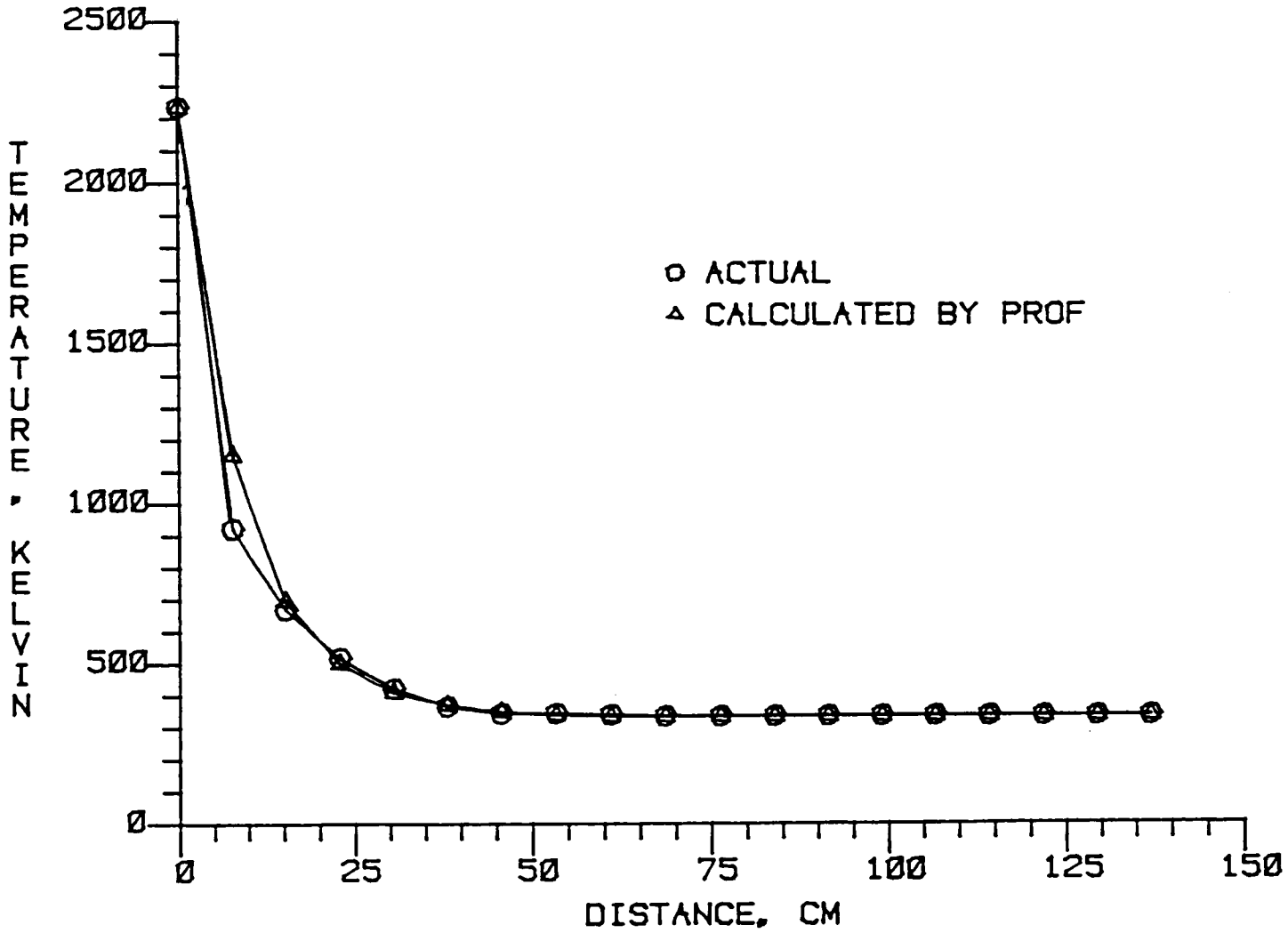

Figure 7. Gas Temperature Profile for Test LMF3B-2b with the Heat Transfer Coefficient Equal to 17.78 W/m^2K.

x and the temperature difference was found to be:

$$\frac{dh}{dx} = \frac{\bar{h}p}{\dot{m}} (T_g - T_w) \tag{13}$$

Finally, substituting equation (9) for the average convective heat transfer coefficient ($\bar{h}$) yielded the following equation:

$$dh = k(T_{gAVG} - T_w) \frac{pNu_D dx}{\dot{m}} \tag{14}$$

The constants in this equation include the wall temperature (T_w), the perimeter (p), the Nusselt number (Nu_D), the mass flow rate ($\dot{m}$), and the tube diameter (D). The enthalpy of the gas in the sample probe was determined using the NASA code. The initial component flow rates used before in tests LMF3B-1 and LMF3B-2b were used except that the components present in the slag were reduced 75 percent to account for losses through the slag tap. The NASA code was then run for the temperatures present in the RF1 sample probe, 300K-2300K. The results of these runs can be found in Figure 8 for tests LMF3B-1 and LMF3B-2b. Another input which varies with the temperature through the sample probe is the thermal conductivity (k). Values for this were found in Reference [7] and were plotted against temperature in Figure 9.

The object of the computer code, which is shown in Appendix C, was to produce a cooling profile through the water cooled sample probe at the RF1 sample location. The interval, dx, was set at 0.01 meters. The temperature, T_{gAVG}, was the average of the initial gas temperature of the specified interval (T_x) and the exit gas temperature of the specified interval (T_{x+dx}). The code initially assumed an exit gas temperature then calculated the change in enthalpy over the interval.

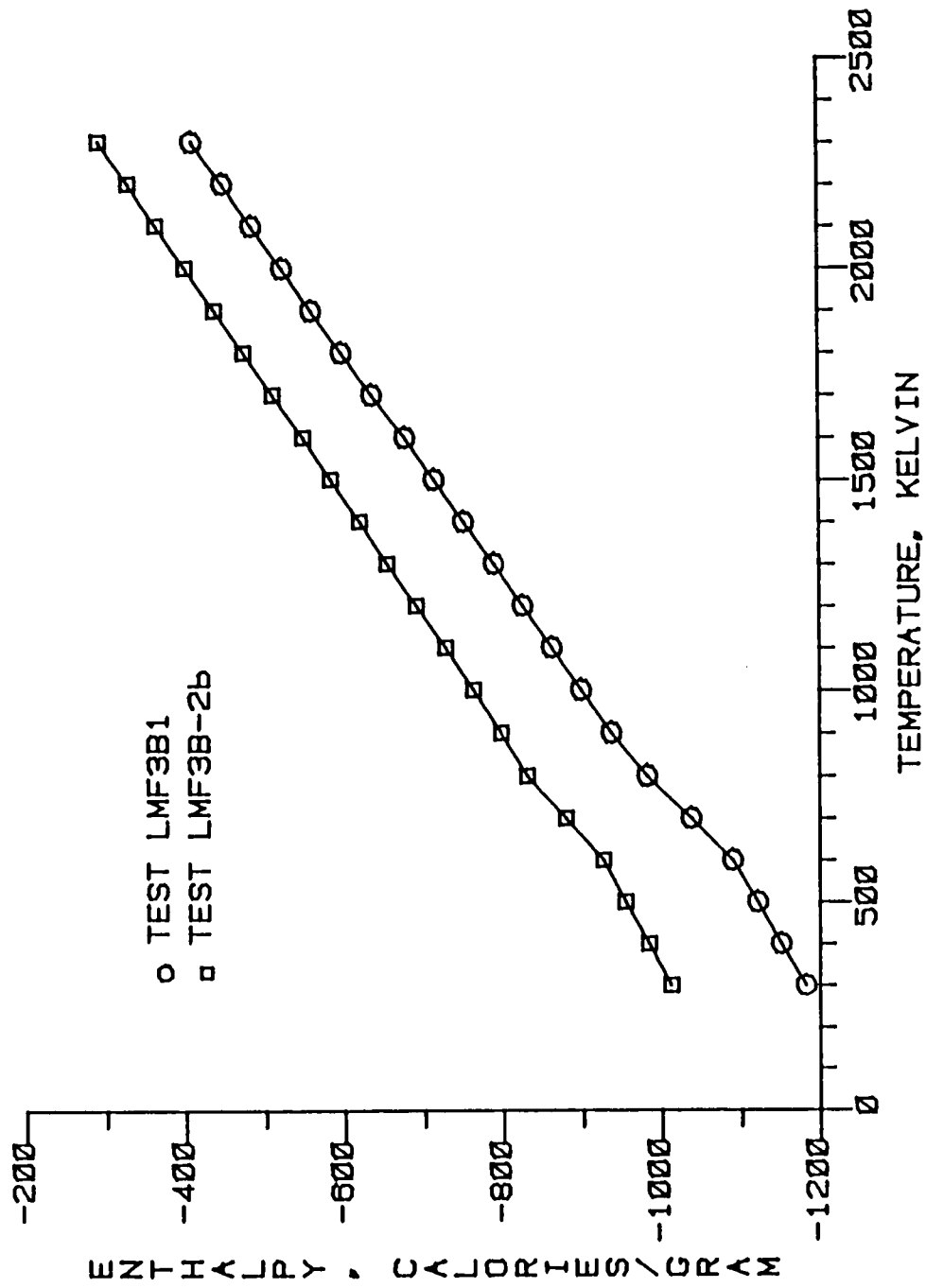

Figure 8. Calculated Enthalpies for the Gas in the RF1 Sample Probe During Tests LMF3B-1 and LMF3B-2b.

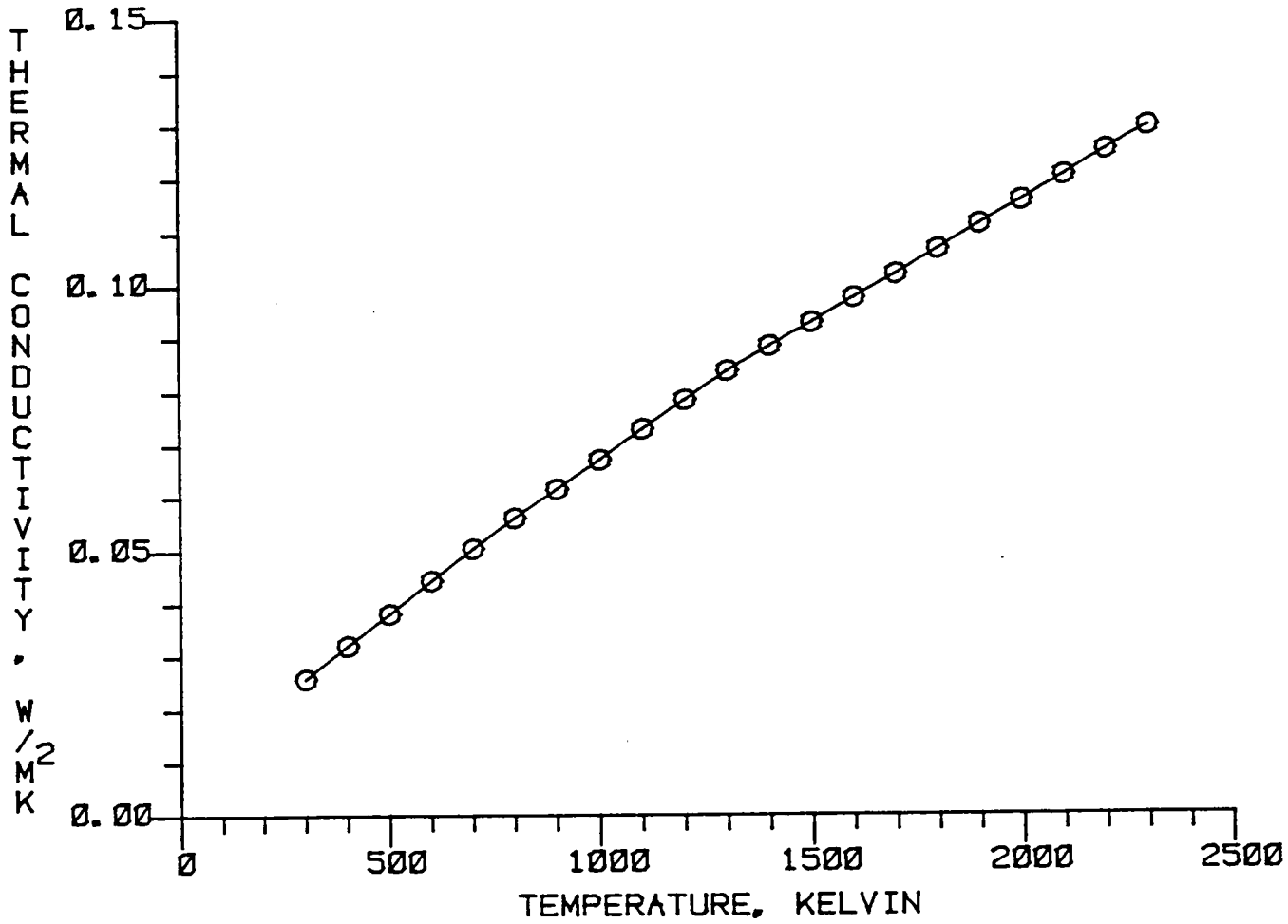

Figure 9. Thermal Conductivity of the Gas for Temperature Range Through the RFI Sample Probe.

Since the initial gas temperature and enthalpy were known, the code could then determine the exit gas enthalpy. This value was then used to determine a new exit gas temperature. The iterative process was continued until the change in the new exit gas temperature was less than 0.1 K. The exit temperature calculated was then used as the initial temperature for the next interval. This process was continued through the length of the sample probe. The temperature profile calculated by this code was then plotted along with the experimentally determined and PROF generated temperature profiles in Figure 10 for test LMF3B-1 and Figure 11 for test LMF3B-2b. The three temperature profiles for the cooling of the gas through the sample probe showed fairly good agreement.

2.5 Determination of Other PROF Inputs

There are several other inputs necessary to run the PROF code with the plug-flow reactor option. The initial temperature of the gas as it enters the sample probe was determined from the program written by Dr. Fred Galanga [4]. Another input parameter that was required was the pressure through the sample probe. This was obtained from the test report from sensors located along the flow train. The values ranged from 0.97 to 1.0 atmospheres. In addition, the ratio of the initial diameter of the sample probe to the mass flow rate was required. The initial area of the sample probe was 11.40 square centimeters while the mass flow rate was determined from Figure 2 (page 10). Another parameter required was the reactor wall temperature. Initially, it was assumed that the reactor or probe was long enough so

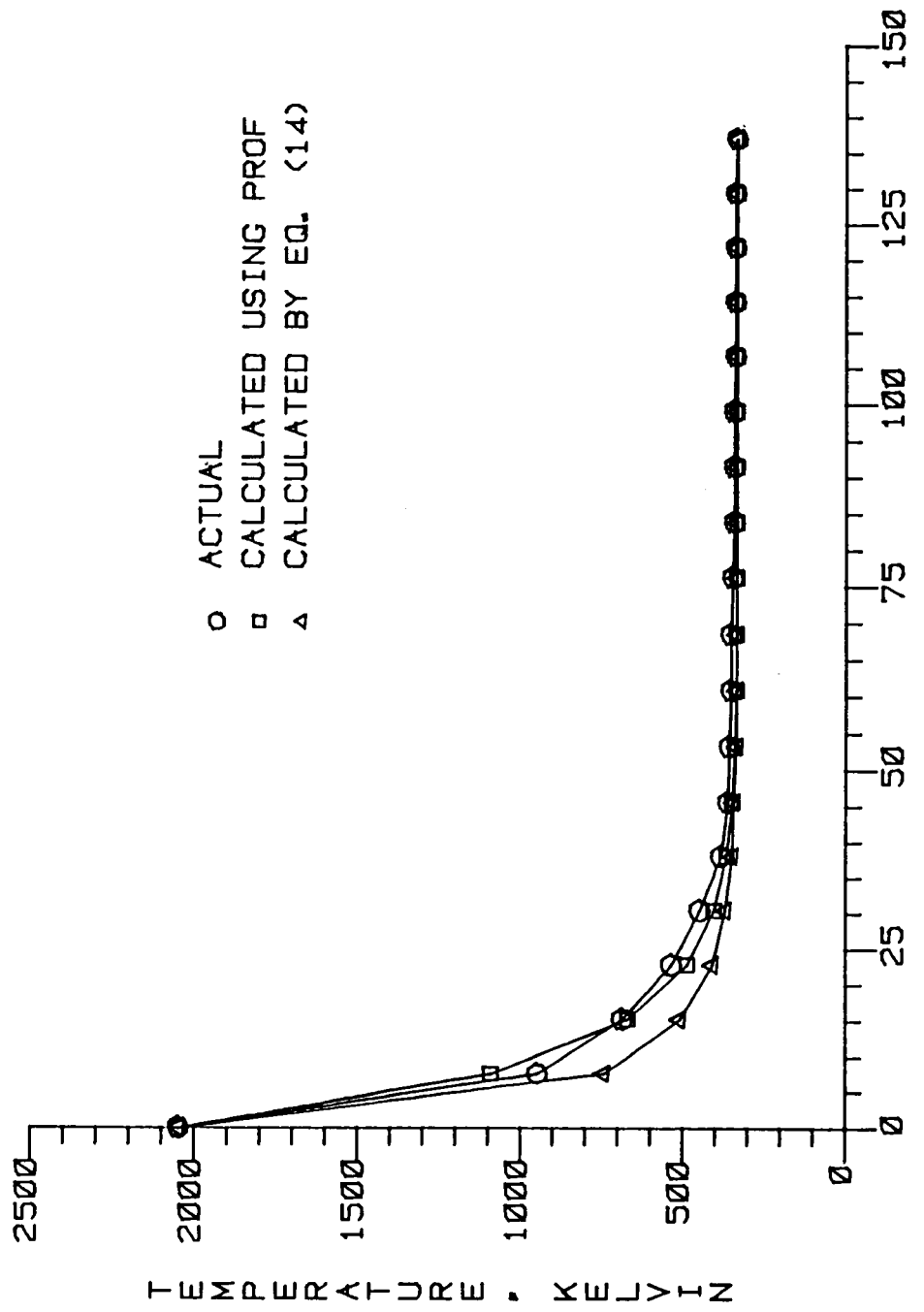

Figure 10. Cooling Profile for the RFI Sample Probe During Test LMF3B-1.

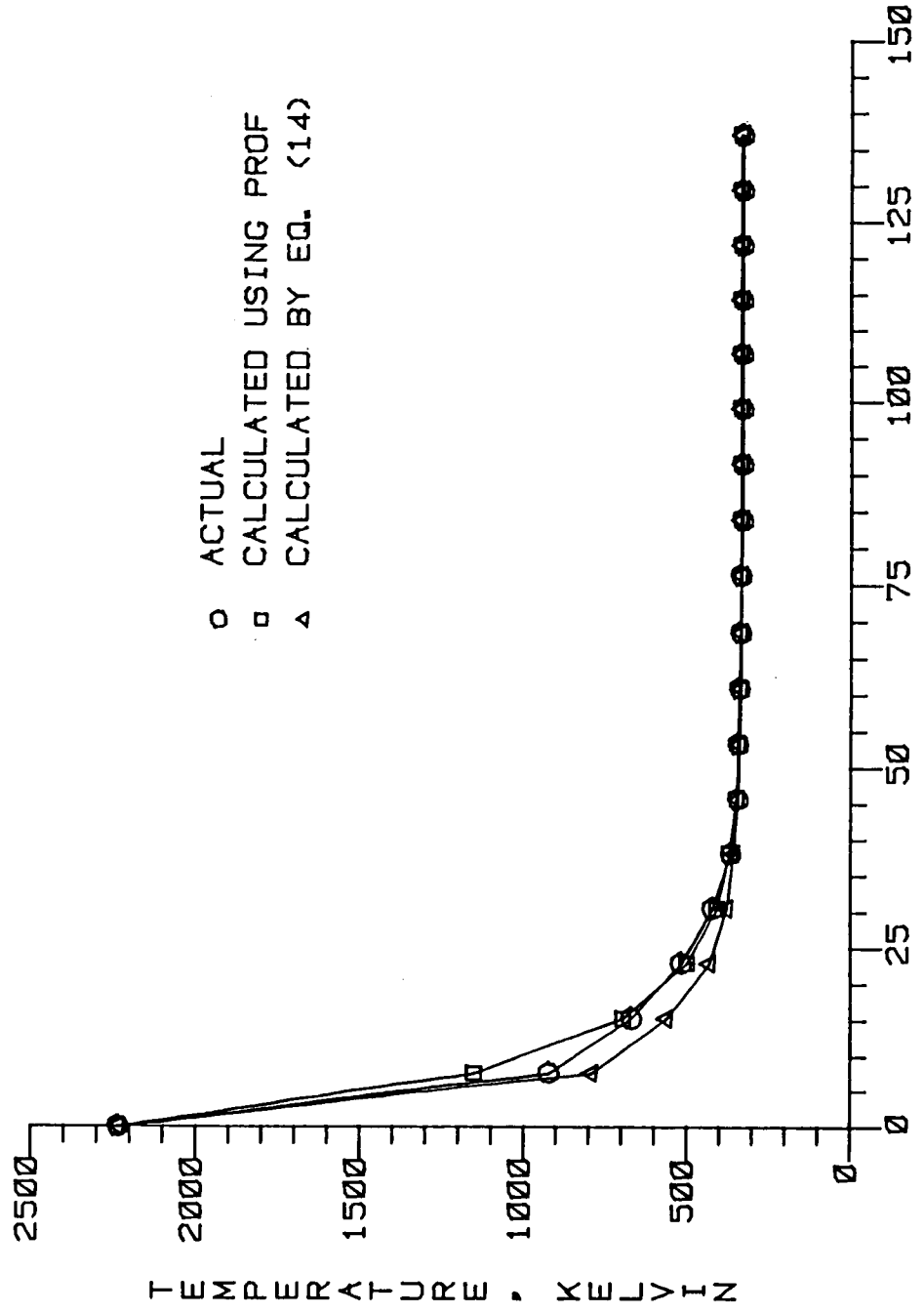

Figure 11. Cooling Profile for the RF1 Sample Probe During Test LMF3B-2b.

that the gas temperature would approach the reactor wall temperature; therefore, the exit gas temperature, 335K, was used as the reactor wall temperature. Later calculations with PROF proved this to be an acceptable assumption. Finally, a reaction set was required to run the code. This reaction set was collected by Dr. Lloyd Crawford and a description can be found in Reference [1]. The reaction set contains 94 reactions that include 30 species containing the elements C, H, N, O, and S.

2.6 Reaction Kinetics Through the Sample Probe

The PROF code with plug-flow option was used to model the kinetics through the sample probes at the RF1 and SCI sample locations. Data from tests LMF3B-1, LMF3B-2a, and LMF3B-2b were used for these runs. For the RF1 location the previously determined heat transfer coefficient, 17.78 W/m^2K, was used to determine the C_j input. At this point the initial temperature was about 2100K while the probe wall temperature was 335K. The results of these runs can be found in Table 1 for test LMF3B-1 and Table 2 for test LMF3B-2b where the initial and final concentrations of the species of interest are listed. These results showed several interesting shifts that occurred through the sample probe. The carbon species showed a slight shift from CO to CO_2. The nitrogen species showed a decomposition of NO while an increase in the NH_3 concentration was seen. The sulfur species showed marked increases in the H_2S and S_2 concentrations while decreases were seen in the SO and HS concentrations.

Table 1. Results from PROF for Test LMF3B-1 at the RF1 Sample Probe.

Species	Initial Concentration (PPM)	Final Concentration (PPM)		% Change
CO	1.1586E+05	1.0498E+05	-	9.3
CO_2	2.0284E+05	2.1413E+05	+	5.6
COH	1.1769E-02	5.5613E-05		--
H	3.3517E+02	3.8556E-08		--
H_2	2.0368E+04	2.9659E+04		--
H_2O	1.6861E+05	1.5980E+05		--
O	3.5826E+00	6.0466E-10		--
O_2	1.2784E+01	1.9812E-05		--
OH	3.0888E+02	1.0921E-12		--
O_2H	6.0109E-03	4.0706E-11		--
N	1.3784E-02	3.3355E-18		--
N_2	4.8483E+05	4.8626E+05		--
NO	2.5691E+03	9.3173E+02	-	63.7
NO_2	2.8596E-02	4.2101E-04		--
N_2O	1.2224E-01	3.5498E-01	+	190.4
NOH	1.5536E-01	8.5719E-01	+	451.7
NH	2.9637E-02	8.1979E-08		--
NH_2	1.1481E-02	3.7637E-08		--
NH_3	2.3578E-01	2.9435E+01	+	12,384.1
CN	2.9030E-05	1.9757E-21		--
HCN	4.9465E-02	5.9899E-02		--
NCO	2.1282E-04	2.0972E-21		--
S	5.6705E+00	4.0492E-03		--
S_2	1.5579E+00	5.9575E+01	+	3,724.1
SO	2.6387E+02	8.2309E-01	-	99.7
SO_2	3.9622E+03	4.0855E+03	+	3.1
SO_3	6.8532E-02	6.7884E-02		--
HS	1.4297E+01	4.3748E-02		--
H_2S	1.2840E+01	6.2008E+01	+	382.9
NS	5.6740E-02	1.7808E-02		--

Table 2. Results From PROF For Test LMF3B-2b at the RF1 Sample Probe.

Species	Initial Concentration (PPM)	Final Concentration (PPM)	% Change
CO	1.1833E+05	1.0668E+05	- 9.8
CO_2	2.0966E+05	2.2190E+05	+ 5.8
COH	2.1466E-02	1.5616E-04	--
H	8.5331E+02	1.5386E-07	--
H_2	1.5284E+04	2.5804E+04	--
H_2O	1.4475E+05	1.3547E+05	--
O	4.5683E+01	2.7854E-11	--
O_2	1.8267E+02	1.8523E-07	--
OH	1.2097E+03	3.0678E-13	--
O_2H	7.1587E-02	5.7182E-12	--
N	2.8818E-02	9.0162E-18	--
N_2	5.0354E+05	5.0484E+05	--
NO	1.0110E+03	1.6498E+02	- 83.7
NO_2	3.2974E-02	1.5860E-05	--
N_2O	2.9393E-02	2.1796E+00	+ 7315.4
NOH	5.3399E-02	5.6598E-01	+ 959.9
NH	1.4786E-02	4.5914E-07	--
NH_2	6.8241E-03	2.4574E-07	--
NH_3	3.9241E-02	5.0179E+01	+127,773.9
CN	1.3153E-05	3.4585E-22	--
HCN	4.7003E-03	2.8465E-02	--
NCO	1.0159E-04	3.9034E-22	--
S	7.5249E+00	1.0960E-02	--
S_2	3.4841E-01	5.5134E+01	+ 15,724.5
SO	3.5254E+02	1.1454E+00	- 99.7
SO_2	4.7606E+03	5.0176E+03	+ 5.4
SO_3	1.9944E-01	1.6522E-01	--
HS	8.3718E+00	3.2196E-02	--
H_2S	3.0120E+00	1.2820E+01	+ 325.6
NS	5.2517E-02	1.7269E-01	--

In order to run the PROF code at the SCI sample location the heat transfer coefficient had to be adjusted for the temperature difference between the two locations. The initial gas temperature at the SCI location is only about 1600K while that at the RF1 location is approximately 2100K. The Nusselt number for the gas flows through the two sample probes were assumed to be the same. Using an average temperature of 970K for the gas in the SCI probe and equation (9) the average heat transfer coefficient was found to be 13.89 W/m^2K. This value was then used to calculate the C_j input for the runs at the SCI sample location. The results of these runs were listed in Table 3 for test LMF3B-2a and Table 4 for test LMF3B-2b. Similar shifts in composition were obtained at the SCI sample location as at the RF1 location. Again the shift from CO to CO_2 was noticed. The same shift from NO to NH_3 was seen for the nitrogen species. The sulfur species showed similar reactions as at the RF1 location except that the H_2S concentration showed a slight decrease rather than an increase. The changes in concentrations seen at the SCI location were not as drastic as those at the RF1 location due to the lesser temperature drop through the SCl sample probe and lower initial temperature.

A point of concern involving the sulfur reactions is the high concentration of sulfur dioxide (SO_2). Through the radiant furnace and up to the secondary combustor reducing conditions exist. This should lead to the reduction of SO_2 to other sulfur species such as sulfur (S_2) and hydrogen sulfide (H_2S). However, the PROF code suggested values of SO_2 about ten times greater than those of H_2S.

Table 3. Results from PROF for Test LMF3B-2a at the SCI Sample Probe.

Species	Initial Concentration (PPM)	Final Concentration (PPM)	% Change
CO	1.0446E+05	1.0203E+05	- 2.3
CO_2	2.0794E+05	2.1039E+05	+ 1.2
COH	1.7763E-03	4.3511E-05	--
H	1.9015E+01	4.4102E-08	--
H_2	2.5322E+04	2.7761E+04	--
H_2O	1.5179E+05	1.4947E+05	--
O	3.2749E-03	1.8897E-13	--
O_2	9.6072E-03	1.4463E-08	--
OH	5.4805E+00	1.9000E-13	--
O_2H	5.2214E-06	2.4599E-13	--
N	2.5984E-04	5.9159E-18	--
N_2	5.0631E+05	5.0634E+05	--
NO	1.1835E+02	8.3252E+01	- 29.7
NO_2	6.1678E-05	1.1289E-08	--
N_2O	2.7402E-03	2.4642E-02	+ 799.3
NOH	9.5740E-03	1.8282E-01	+ 1809.6
NH	1.0869E-03	7.8816E-09	--
NH_2	1.0064E-02	1.6736E-07	--
NH_3	5.3937E+00	1.8380E+01	+ 260.0
CN	3.8302E-07	2.7762E-22	--
HCN	4.0758E-02	4.0835E-02	--
NCO	2.8043E-06	3.1022E-22	--
S	2.6874E-00	3.2129E-03	--
S_2	1.0430E+02	2.3390E+02	+ 125.0
SO	1.4147E+02	9.5400E-01	- 99.3
SO_2	3.3790E+03	3.4109E+03	+ 1.0
SO_3	1.9319E-02	1.9306E-02	--
HS	4.4779E+01	8.5958E-02	--
H_2S	3.6011E+02	2.5717E+02	- 28.6
NS	1.3883E-02	1.0891E-03	--

Table 4. Results from PROF for Test LMF3B-2b at the SCI Sample Probe.

Species	Initial Concentration (PPM)	Final Concentration (PPM)	% Change
CO	1.0849E+05	1.0602E+05	- 2.3
CO_2	2.2026E+05	2.2274E+05	+ 1.1
COH	1.7008E-03	4.7351E-05	--
H	1.5945E+01	4.9627E-08	--
H_2	2.2160E+04	2.4644E+04	--
H_2O	1.3885E+05	1.3652E+05	--
O	2.4351E-03	5.7335E-14	--
O_2	7.0681E-03	5.8124E-09	--
OH	4.2108E+00	1.7550E-13	--
O_2H	3.5038E-06	1.3585E-13	--
N	2.0633E-04	6.9829E-18	--
N_2	5.0515E+05	5.0518E+05	--
NO	9.2380E+01	6.5241E+01	- 29.4
NO_2	3.8131E-05	5.7820E-09	--
N_2O	2.3067E-03	1.3005E-02	+ 463.8
NOH	8.1350E-03	1.2964E-01	+1,493.6
NH	1.0281E-03	5.9893E-09	--
NH_2	1.0171E-02	1.6475E-07	--
NH_3	5.7705E+00	1.6686E+01	+ 189.2
CN	3.0448E-07	2.5922E-22	--
HCN	3.6885E-02	3.6943E+02	--
NCO	2.2497E-06	2.9751E-22	--
S	3.1352E+00	3.3500E-03	--
S_2	1.7316E+02	3.2891E+02	+ 89.9
SO	1.6752E+02	9.9739E-01	- 99.4
SO_2	4.1914E+03	4.2246E+03	+ 0.8
SO_3	2.4200E-02	2.4188E-02	--
HS	4.9493E+01	8.9548E-02	--
H_2S	3.8675E+02	2.6134E+02	- 32.4
NS	1.7415E-02	7.7822E-04	--

Due to inherent limitations of the PROF code, mole fractions less than 10^{-27} cannot be handled. This created problems with the runs at both sample locations. Some of the lesser species were reaching values below this limit before the end of the sample probe which is 137 centimeters long. The maximum distance into the probe that PROF could be run was 38.1 centimeters at the RF1 sample location and 24 centimeters at the SCI sample location. However, at these distances the major constituents in the gas had reached a steady state composition and it was assumed that no further change would occur through the remainder of the probe.

The previously discussed runs were carried out with the conditions as close as possible to the actual test conditions. Furthur runs were done with the major inputs of the PROF code altered to determine the effect on the reactions through the sample probe. Initially, the mass flow rate through the sample probe at the SCI location was reduced one half. This increased the ratio of the initial area to the mass flow rate. The results of this run and the previous run were listed in Table 5 for test LMF3B-2a and Table 6 for test LMF3B-2b. Again some of the lesser species in the gas stream became too small for the PROF code to handle; therefore, the run could only be used 12 centimeters into the probe. Even so, the major constituents in the gas stream were within 1 percent of the values for the control run. The lesser species showed quite a large variance from the values determined using the actual mass flow rate. This is due to the higher temperatures and shorter residence time in the probe

Table 5. Results from PROF with Reduced Mass Flow Rate for Test LMF3B-2a.

Species	Final Concentrations: Actual Mass Flow Rate (PPM)	Final Concentrations: 1/2 Actual Mass Flow Rate (PPM)	% Difference
CO	1.0203E+05	1.0233E+05	+ 0.3
CO_2	2.1039E+05	2.1008E+05	- 0.1
COH	4.3511E-05	6.2848E-05	+ 44.4
H	4.4102E-08	2.3196E-07	+ 426.0
H_2	2.7761E+04	2.7473E+04	- 1.0
H_2O	1.4947E+05	1.4976E+05	+ 0.2
O	1.8897E-13	2.5582E-12	+1253.8
O_2	1.4463E-08	1.4747E-07	+ 919.6
OH	1.9000E-13	1.2187E-12	+ 541.4
O_2H	2.4599E-13	2.9212E-12	+1087.5
N	5.9159E-18	6.4834E-17	+ 995.9
N_2	5.0634E+05	5.0634E+05	0.0
NO	8.3252E+01	8.2884E+01	0.4
NO_2	1.1289E-08	4.9741E-08	+ 340.6
N_2O	2.4642E-02	2.4515E-02	- 0.5
NOH	1.8282E-01	1.8497E-01	+ 1.2
NH	7.8816E-09	1.9195E-08	+ 143.5
NH_2	1.6736E-07	4.1145E-07	+ 145.8
NH_3	1.8380E+01	1.8584E+01	+ 1.1
CN	2.7762E-22	2.5630E-21	+ 823.2
HCN	4.0835E-02	4.0802E-02	0.1
NCO	3.1022E-22	3.3026E-21	+ 964.6
S	3.2129E-03	4.1562E-03	+ 29.4
S_2	2.3390E+02	2.2718E+02	- 2.9
SO	9.5400E-01	1.1587E+00	+ 21.5
SO_2	3.4109E+03	3.4219E+03	+ 0.3
SO_3	1.9306E-02	1.9316E-02	+ 0.1
HS	8.5958E-02	1.2285E-01	+ 42.9
H_2S	2.5717E+02	2.5934E+02	+ 0.8
NS	1.0891E-03	1.2749E-03	+ 17.1

Table 6. Results from PROF with Reduced Mass Flow Rate for Test LMF3B-2b.

Species	Final Concentrations: Actual Mass Flow Rate (PPM)	Final Concentrations: 1/2 Actual Mass Flow Rate (PPM)	% Difference
CO	1.0602E+05	1.0647E+05	+ 0.4
CO_2	2.2274E+05	2.2229E+05	- 0.2
COH	4.7351E-05	6.8419E-05	+ 44.5
H	4.9627E-08	2.5726E-07	+ 418.4
H_2	2.4644E+04	2.4213E+04	- 1.8
H_2O	1.3652E+05	1.3694E+05	+ 0.3
O	5.7335E-14	8.6650E-13	+1411.3
O_2	5.8124E-09	6.6256E-08	+1040.0
OH	1.7550E-13	1.1049E-12	+ 529.6
O_2H	1.3585E-13	1.7978E-12	+1223.4
N	6.9829E-18	7.5046E-17	+ 974.7
N_2	5.0518E+05	5.0518E+05	0.0
NO	6.5241E+01	6.5347E+01	+ 0.2
NO_2	5.7820E-09	2.3533E-08	+ 307.0
N_2O	1.3005E-02	1.3027E-02	+ 0.2
NOH	1.2964E-01	1.3080E-01	+ 0.9
NH	5.9893E-09	1.4378E-08	+ 140.1
NH_2	1.6475E-07	4.0059E-07	+ 143.2
NH_3	1.6686E+01	1.6682E+01	+ 0.0
CN	2.5922E-22	2.3371E-21	+ 801.6
HCN	3.6943E-02	3.6917E-02	+ 0.1
NCO	2.9751E-22	3.0829E-21	+ 936.2
S	3.3500E-03	4.3347E-03	+ 29.4
S_2	3.2891E+02	3.2012E+02	- 2.7
SO	9.9739E-01	1.2173E+00	+ 22.0
SO_2	4.2246E+03	4.2371E+03	+ 0.3
SO_3	2.4188E-02	2.4198E-02	0.0
HS	8.9548E-02	1.2833E-01	+ 43.3
H_2S	2.6134E+02	2.6609E+02	+ 1.8
NS	7.7822E-04	9.1245E-04	+ 17.3

at the point examined. Most of the lesser species are only present at higher temperatures and as the temperature drops through the probe these less stable species shift to the more stable constituents in the gas stream. The residence time for this run was 2.0 seconds through twelve centimeters while the previous run was through 24 centimeters and required 2.2 seconds.

Next, the mass flow rate through the sample probe at the SCI sample location was doubled. This decreased the ratio of the initial area to the mass flow rate. These results were tabulated in Table 7 for test LMF3B-2a and Table 8 for test LMF3B-2b. With the accelerated flow rate the PROF code could be used 46 centimeters into the sample probe. Again, the major constituents in the gas stream were within one percent of the run with the normal mass flow rate. The lesser species showed better agreement with the control run than was seen with one half the mass flow rate. It was evident that the longer distance in the probe allowed slightly more decomposition of the unstable intermediate species. Also, a slightly lower temperature was seen after 46 centimeters in the probe even with the accelerated flow rate.

From this analysis it was determined that the mass flow rate of the gas through the sample probe had little effect on the extent or nature of reactions in the probe. Hence, variations in the pressure across the eductor should not affect the final composition of the gas to be analyzed. The mass flow rate does influence the distance into the probe that the reactions occur. In addition, the area of the

Table 7. Results from PROF with Increased Mass Flow Rate for Test LMF3B-2a.

Species	Final Concentrations: Actual Mass Flow Rate (PPM)	Final Concentrations: Twice Actual Mass Flow Rate (PPM)	% Difference
CO	1.0203E+05	1.0196E+05	- 0.1
CO_2	2.1039E+05	2.1046E+05	+ 0.0
COH	4.3511E-05	4.0752E-05	- 6.3
H	4.4102E-08	3.5978E-08	- 18.4
H_2	2.7761E+04	2.7823E+04	+ 0.2
H_2O	1.4947E+05	1.4941E+05	+ 0.0
O	1.8897E-13	5.6717E-14	- 70.0
O_2	1.4463E-08	4.6386E-09	- 67.9
OH	1.9000E-13	1.5185E-13	- 20.1
O_2H	2.4599E-13	7.5231E-14	- 69.4
N	5.9159E-18	4.4940E-18	- 24.0
N_2	5.0634E+05	5.0634E+05	+ 0.0
NO	8.3252E+01	8.3713E+01	+ 0.6
NO_2	1.1289E-08	6.7711E-09	- 40.0
N_2O	2.4642E-02	2.4078E-02	- 2.3
NOH	1.8282E-01	1.8308E-01	+ 0.1
NH	7.8816E-09	7.0518E-09	- 10.5
NH_2	1.6736E-07	1.4849E-07	- 11.3
NH_3	1.8380E+01	1.8113E+01	- 1.5
CN	2.7762E-22	2.1332E-22	- 23.2
HCN	4.0835E-02	4.0857E-02	+ 0.1
NCO	3.1022E-22	2.3486E-22	- 24.2
S	3.2129E-03	3.0446E-03	- 5.2
S_2	2.3390E+02	2.3701E+02	+ 1.3
SO	9.5400E-01	9.1537E-01	- 4.1
SO_2	3.4109E+03	3.4056E+03	- 0.2
SO_3	1.9306E-02	1.9295E-02	- 0.1
HS	8.5958E-02	8.1560E-02	- 5.1
H_2S	2.5717E+02	2.5628E+02	- 0.4
NS	1.0891E-03	1.0058E-03	- 7.7

Table 8. Results from PROF with Increased Mass Flow Rate for Test LMF3B-2b.

Species	Final Concentrations: Actual Mass Flow Rate (PPM)	Final Concentrations: Twice Actual Mass Flow Rate (PPM)	% Difference
CO	1.0602E+05	1.0585E+05	- 0.2
CO_2	2.2274E+05	2.2292E+05	+ 0.1
COH	4.7351E-05	4.9907E-05	+ 5.4
H	4.9627E-08	7.8548E-08	+ 58.3
H_2	2.4644E+04	2.4810E+04	+ 0.7
H_2O	1.3652E+05	1.3635E+05	- 0.1
O	5.7335E-14	2.1668E-14	- 62.2
O_2	5.8124E-09	2.1726E-09	- 62.6
OH	1.7550E-13	3.0070E-13	+ 71.3
O_2H	1.3585E-13	4.9836E-14	- 63.3
N	6.9828E-18	1.4202E-17	+ 103.4
N_2	5.0518E+05	5.0518E+05	+ 0.0
NO	6.5241E+01	6.5374E+01	+ 0.2
NO_2	5.7820E-09	3.7058E-09	- 35.9
N_2O	1.3005E-02	1.2411E-02	- 4.6
NOH	1.2964E-01	1.3073E-01	+ 0.8
NH	5.9893E-09	7.6900E-09	+ 28.4
NH_2	1.6475E-07	2.0884E-07	+ 26.8
NH_3	1.6686E+01	1.6553E+01	- 0.8
CN	2.5922E-22	4.9969E-22	+ 92.8
HCN	3.6943E-02	3.6960E-02	+ 0.1
NCO	2.9751E-22	6.0193E-22	+ 102.3
S	3.3500E-03	3.4316E-03	+ 2.4
S_2	3.2891E+02	3.3336E+02	+ 1.4
SO	9.9739E-01	1.0131E+00	+ 1.6
SO_2	4.2246E+03	4.2181E+03	- 0.2
SO_3	2.4188E-02	2.4177E-02	- 0.1
HS	8.9548E-02	9.6746E-02	+ 8.0
H_2S	2.6134E+02	2.5893E+02	- 0.9
NS	7.7822E-04	7.2542E-04	- 6.8

probe has little effect on the extent of the reactions since altering the ratio of the initial area to the mass flow rate did not alter the final gas composition.

2.7 Examination of Solids Precipitating in the Sample Probe

The PROF code considers that only gaseous species are present in the sample probe. At the temperatures reached in the lower portion of the sample probe some of the species may begin to precipitate as solids. These condensed species could affect the reactions which occur through the sample probe. In order to examine when these precipitates begin to appear the NASA equilibrium code was used. Input data for Tests LMF3B-1 and LMF3B-2b were used in this analysis. The same input used to determine the gas composition at the radiant furnace entrance was used except that the constituents present in the ash were reduced 75 percent to account for losses through the slag tap. This should give a better representation of the actual gas in the sample probe. The NASA code was then run for temperatures from 2250K to 300K at 50K intervals.

In order to evaluate the data the change in enthalpy versus temperature was analyzed. The enthalpy of a mixture can be expressed:

$$h = \sum n_i H_i \tag{15}$$

Then, the change in enthalpy as temperature changes at constant pressure becomes:

$$\frac{\partial h}{\partial T} = \sum n_i \frac{\partial H_i}{\partial T} + \sum H_i \frac{\partial n_i}{\partial T} \tag{16}$$

Finally, since $\partial H_i/\partial T = C_{pi}$ the equation becomes

$$\frac{\partial h}{\partial T} = \sum C_{pi} n_i + \sum H_i \frac{\partial n_i}{\partial T} \tag{17}$$

As long as the phase of the species present remains consistent the heat capacity and enthalpy should exhibit consistent changes with temperature. However, when a precipitate forms or changes from one species to another occurs, it will be reflected in the heat capacity and enthalpy.

The heat capacity and enthalpy were plotted against temperature in Figure 12 for Test LMF3B-1 and Figure 13 for Test LMF3B2-2b. In addition, the concentration of the solid species of interest are listed in Tables 9 and 10 for the two test runs. Examination of the data reveals the first inconsistency in the heat capacity and enthalpy at 1400K. At this point liquid potassium sulfide (K_2S) first appears. At 950K the potassium sulfide dissociates and the potassium carbonate (K_2CO_3) is formed. Finally, in the temperature range of 650-800K several phenomena occur which cause fluctuations in the heat capacity and enthalpy. The crystalline structure of sodium carbonate (Na_2CO_3) changes while potassium silicate (K_2SiO_3) dissociates and forms silicon dioxide (SiO_2). Above 1600K the heat capacity and enthalpy did not show the inconsistencies seen in the previously discussed figures.

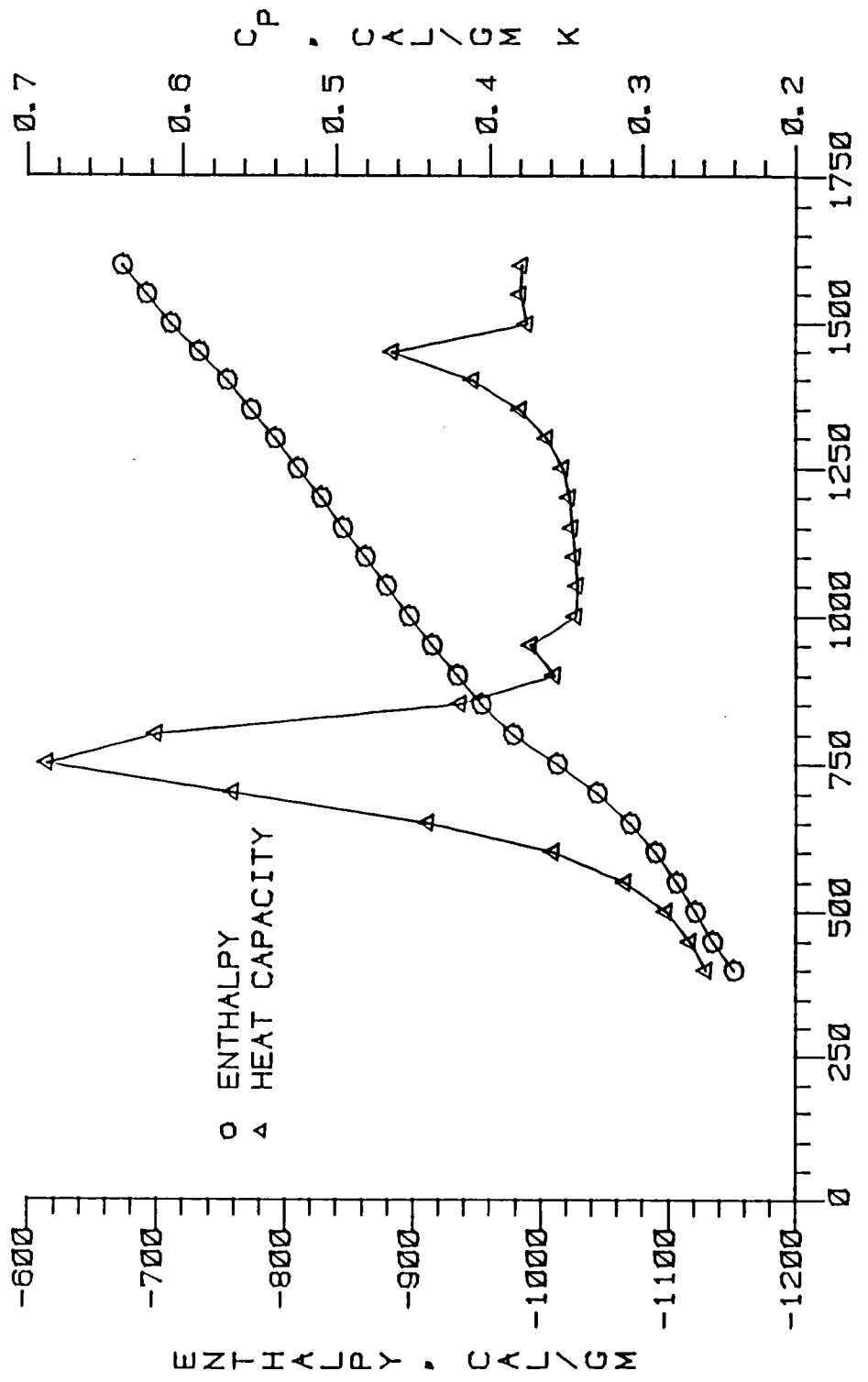

Figure 12. Enthalpy and Heat Capacity of the Sample Gas Predicted by NASA for Test LMF3B-1.

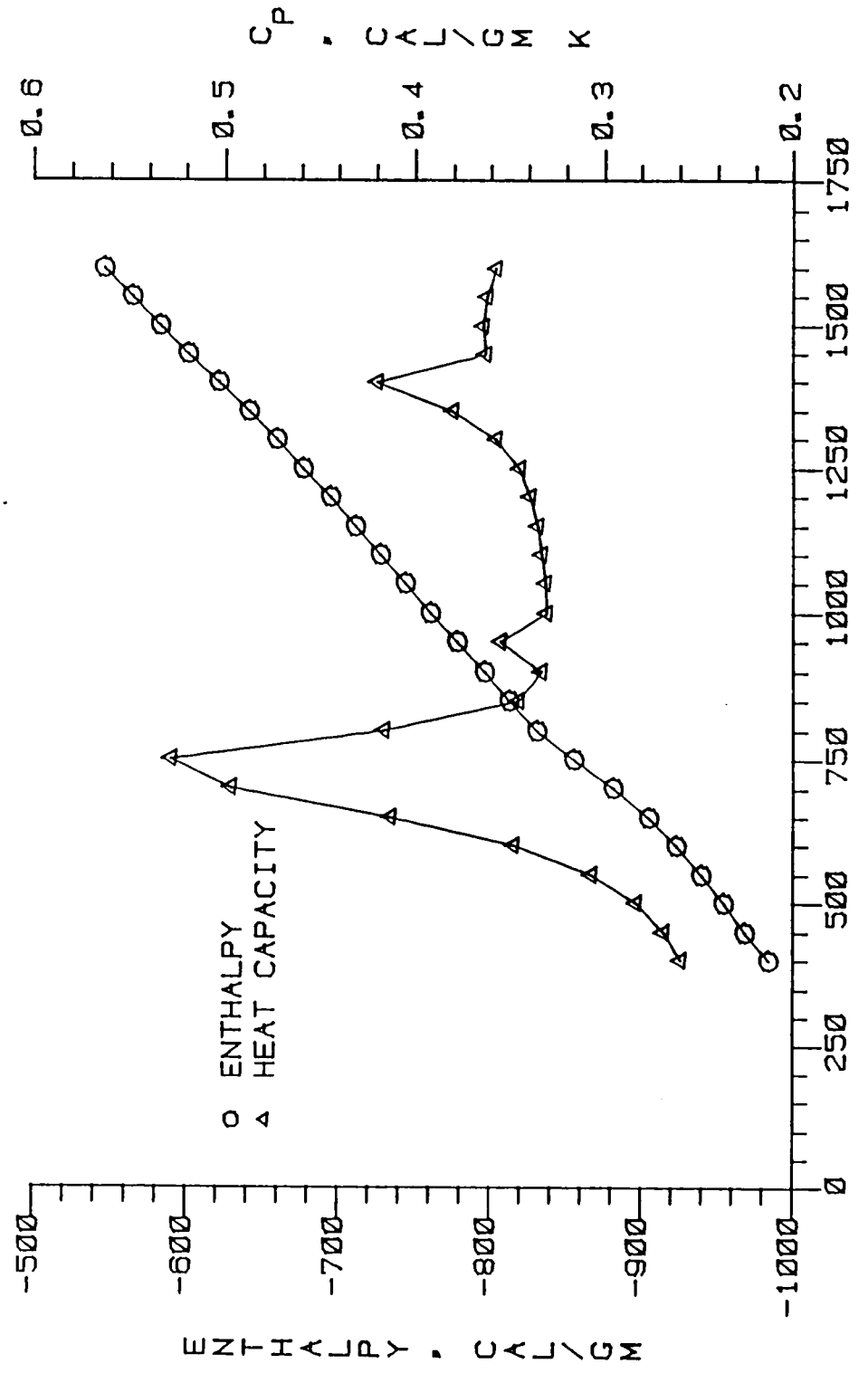

Figure 13. Enthalpy and Heat Capacity of the Sample Gas Predicted by NASA for Test LMF3B-2b.

Table 9. Precipitates in the Sample Probe Predicted with NASA Code for Test LMF3B-1.

TEMP.	K_2S(L)	K_2S(S1)	K_2S(S2)	K_2CO_3(S)	Na_2CO_3(S2)	Na_2CO_3(S1)	K_2SiO_3	SiO_2(S)
1600	--	--	--	--	--	--	--	--
1550	--	--	--	--	--	--	--	--
1500	--	--	--	--	--	--	--	--
1450	--	--	--	--	--	--	--	--
1400	614.3	--	--	--	--	--	--	--
1350	1292.2	--	--	--	--	--	--	--
1300	1686.8	--	--	--	--	--	--	--
1250	1911.1	--	--	--	--	--	--	--
1200	--	2033.7	--	--	--	--	572.6	--
1150	--	2095.3	--	--	--	--	572.6	--
1100	--	2122.6	--	--	4.2	--	572.6	--
1050	--	--	2133.4	--	6.0	--	572.6	--
1000	--	--	2137.3	--	6.4	--	572.6	--
950	--	--	1244.3	896.4	6.5	--	573.2	--
900	--	--	--	2143.7	6.5	--	573.9	--
850	--	--	--	2144.4	6.5	--	574.1	--
800	--	--	--	2149.0	6.6	--	575.3	--
750	--	--	--	2166.6	6.6	--	580.0	--
700	--	--	--	2192.4	--	6.7	586.9	--
650	--	--	--	2805.5	--	6.8	--	592.4
600			-	2822.1	--	6.8	--	596.0
550	--	--	--	2831.4	--	6.8	--	597.9
500	--	--	--	2836.2	--	6.8	--	598.9
450	--	--	--	2838.1	--	6.8	--	599.3
400	--	--	--	--	--	6.9	--	601.2

*Concentrations in PPM

Table 10. Precipitates in the Sample Probe Predicted with NASA Code for Test LMF3B-2b.

TEMP.	K_2S(L)	K_2S(S1)	K_2S(S2)	K_2CO_3(S)	Na_2CO_3(S2)	Na_2CO_3(S1)	K_2SiO_3	SiO_2(S)
1600	--	--	--	--	--	--	--	--
1550	--	--	--	--	--	--	--	--
1500	--	--	--	--	--	--	--	--
1450	661.8	--	--	--	--	--	--	--
1400	1678.8	--	--	--	--	--	--	--
1350	2259.9	--	--	--	--	--	--	--
1300	2662.8	--	--	--	--	--	--	--
1250	2871.4	--	--	--	--	--	--	--
1200	--	2983.7	--	--	--	--	878.8	--
1150	--	3038.9	--	--	--	--	878.8	--
1100	--	3062.9	--	--	6.9	--	878.8	--
1050	--	--	3072.4	--	8.7	--	878.8	--
1000	--	--	3075.8	--	9.1	--	878.8	--
950	--	--	2428.1	650.9	9.2	--	879.4	--
900	--	--	--	3087.5	9.2	--	881.8	--
850	--	--	--	3092.5	9.2	--	883.2	--
800	--	--	--	3118.1	9.3	--	890.5	--
750	--	--	--	3173.6	9.5	--	906.3	--
700	--	--	--	3229.6	--	9.6	922.3	--
650	--	--	--	4200.9	--	9.8	--	933.2
600	--	--	--	4229.8	--	9.8	--	939.6
550	--	--	--	4245.1	--	9.9	--	943.0
500	--	--	--	4253.2	--	9.9	--	944.8
450	--	--	--	4256.2	--	9.9	--	945.5
400	--	--	--	--	--	9.9	--	949.8

*Concentrations in PPM

3.0 EXPERIMENTAL ANALYSIS

3.1 Determination of Trace Nitrogen Species

From the theoretical analysis using the PROF code it was determined that NO was shifting to other nitrogen species as the gas passed through the sample probe. This prompted an effort to experimentally determine the concentration in the actual sample gas of ammonia and hydrogen cyanide. A literature search was conducted to find the most reliable method of determining these compounds in a combustion gas sample. Most articles found suggested the use of ion selective electrodes in the analysis [8,9,10]. This method involved bubbling the sample gas through acidic and basic solutions where the compounds of interest would be absorbed, then determining the concentrations in these samples using the ion-specific electrodes. A 0.2 percent H_2SO_4 solution was used to absorb the NH_3 while a 0.5 N NaOH solution absorbed the HCN. An air flow meter was used to monitor the amount of sample gas that was bubbled through the solutions. The solutions were contained in 500 ml glass impingers and special glass inserts fitted with sandstones were used to guarantee efficient contact of the combustion gas with the liquid. A schematic diagram of the sampling apparatus is shown in Figure 14.

Samples for ammonia and cyanide analysis were taken during tests LMF3B-2a and LMF3B-2b from the SCI sample location. One sample was collected during test LMF3B-2a at 8:50 where 4.7 cubic feet of combustion gas were bubbled through the solutions in 14.5 minutes.

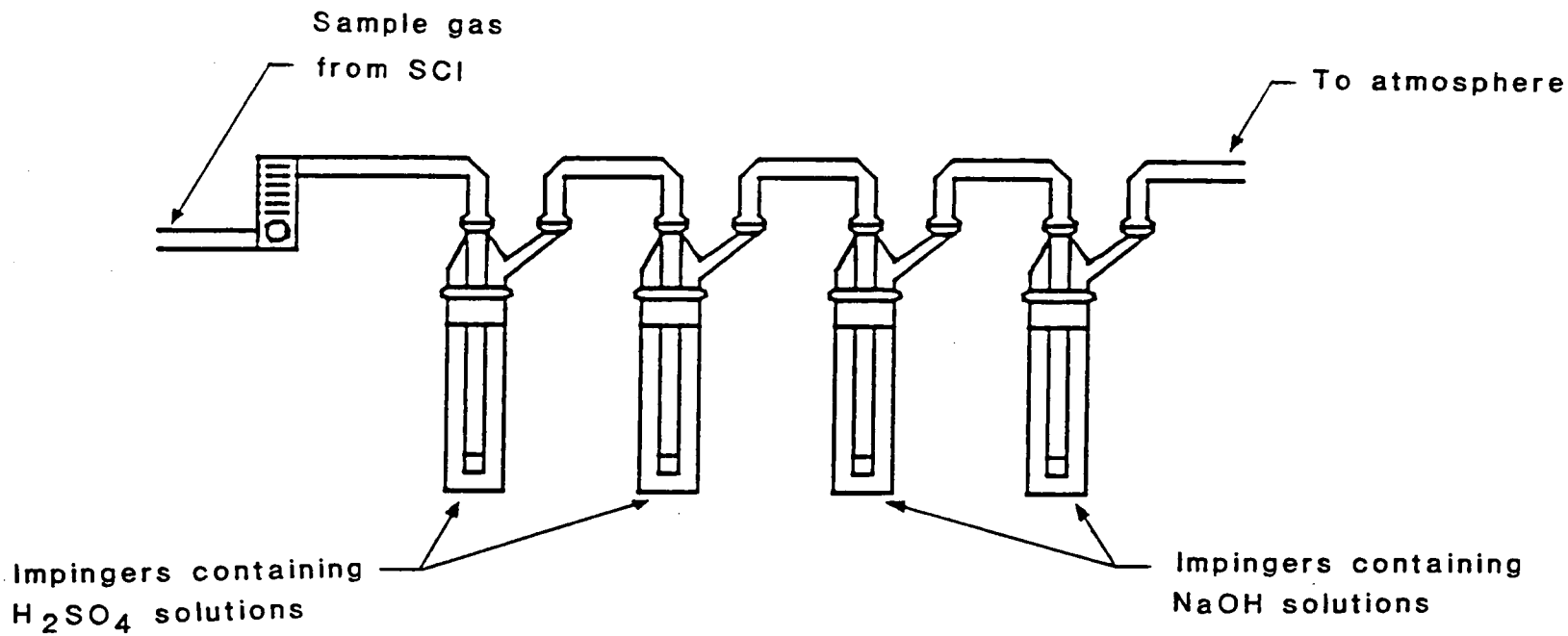

Figure 14. Schematic Diagram of the Flow Train Used to Collect Ammonia and Hydrogen Cyanide Samples.

During test LMF3B-2b three "bubble samples" were collected. At 8:07 five cubic feet of combustion gas were bubbled through four impingers containing only the H_2SO_4 solution in 19 minutes. Then at 9:50 five cubic feet of combustion gas were bubbled through four impingers containing only the NaOH solution in 25 minutes. A final sample was collected at 12:02 where five cubic feet of combustion gas were bubbled through both solutions in 40 minutes. The first two samples were taken to see if the additional residence time in the solutions would cause a significant increase in the observed species concentration as compared to those in the final sample. In addition, a bag sample was collected before each "bubble sample" was taken which was later analyzed for hydrogen sulfide (H_2S) on a gas chromatograph.

3.1.1 Ammonia Analysis. The ammonia was measured using an Orion 95-12 NH_3 gas-sensing electrode. The relative potential of this electrode was monitored using an Orion Model 701A digital pH/mV meter. In the solution the NH3 species actually existed as NH_4^+. The NH_4^+ was converted to NH_3 immediately prior to analysis by adding 1 ml of 10 M NaOH. Standard solutions of NH_3 were prepared using reagent grade ammonium chloride (NH_4Cl). A calibration curve prepared immediately prior to analysis of the samples is shown in Figure 15. A 100-ml aliquot of the sample was analyzed to determine the concentration of NH_3 in the liquid sample. This was then converted to the PPM of NH_3 present in the dry sample gas. The results can be found in Table 11.

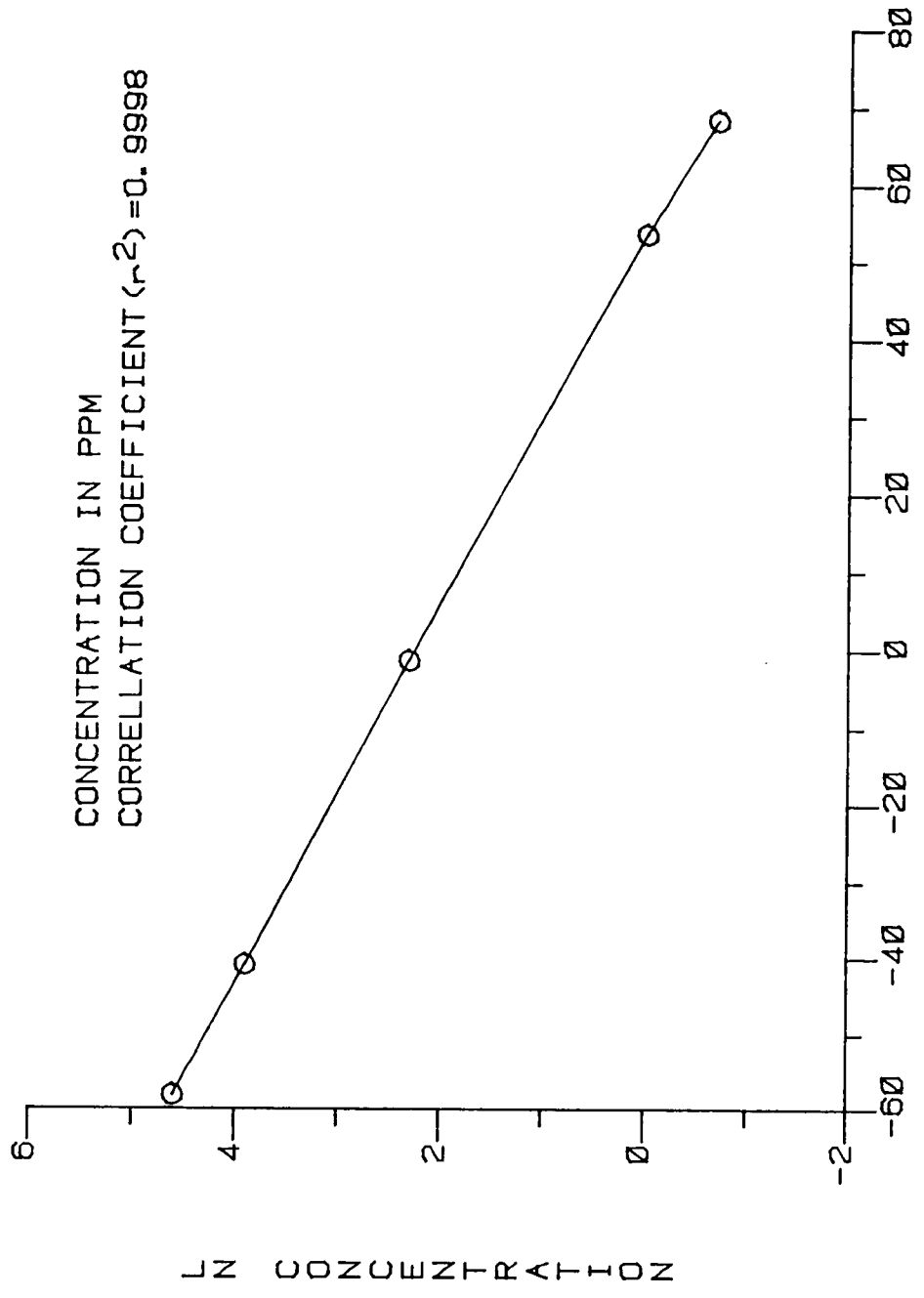

Figure 15. Calibration Curve for the Ammonia Gas-sensing Electrode.

Table 11. Results of Ammonia Analysis

Sample No.	Test	Time	NH_3 Concentration (PPM Dry Gas)
1	LMF3B-2a	8:50 A.M.	12.4
2	LMF3B-2b	8:07 A.M.	25.6
3	LMF3B-2b	9:50 A.M.	-
4	LMF3B-2b	12:02 P.M.	28.3

3.1.2 Cyanide Analysis. Cyanide was measured using an Orion Model 94-06 CN^- specific electrode with an Orion Model 90-02 double junction reference electrode. Again, the Orion Model 701A digital pH/mV meter was used to monitor the relative potential. The standard cyanide solutions were prepared using dry, reagent grade sodium cyanide (NaCN). A calibration curve prepared immediately prior to analysis of the cyanide samples is shown in Figure 16.

The initial analysis of the cyanide samples yielded values which were between 20-30 PPM CN^- dry gas. These values were 2000-3000 times too high according to the theoretical analysis. It was determined that the sulfide ion (S^{2-}) was present in the solution and that it was reacting with the cyanide specific electrode and causing the erroneous readings. The instruction manual for the cyanide electrode stated that the sulfide ion must be absent from the solution for correct cyanide analysis. A weak solution of lead nitrate ($Pb(NO_3)_2$) was added to the sample which should have formed lead sulfide (PbS), a black precipitate [11]. However, a white precipitate was formed. The instruction manual for the silver/sulfide electrode, which can also be used for cyanide detection in dilute solutions, suggested using cadmium nitrate ($Cd(NO_3)_2$) to precipitate the sulfide ions. Again, a white precipitate was noticed while cadmium sulfide (CdS) is a yellow-orange color. It was determined that the white precipitates formed were the carbonates of the respective cations. Hence, the sulfide ions could not be removed from the samples and a correct reading for the cyanide samples could not be determined.

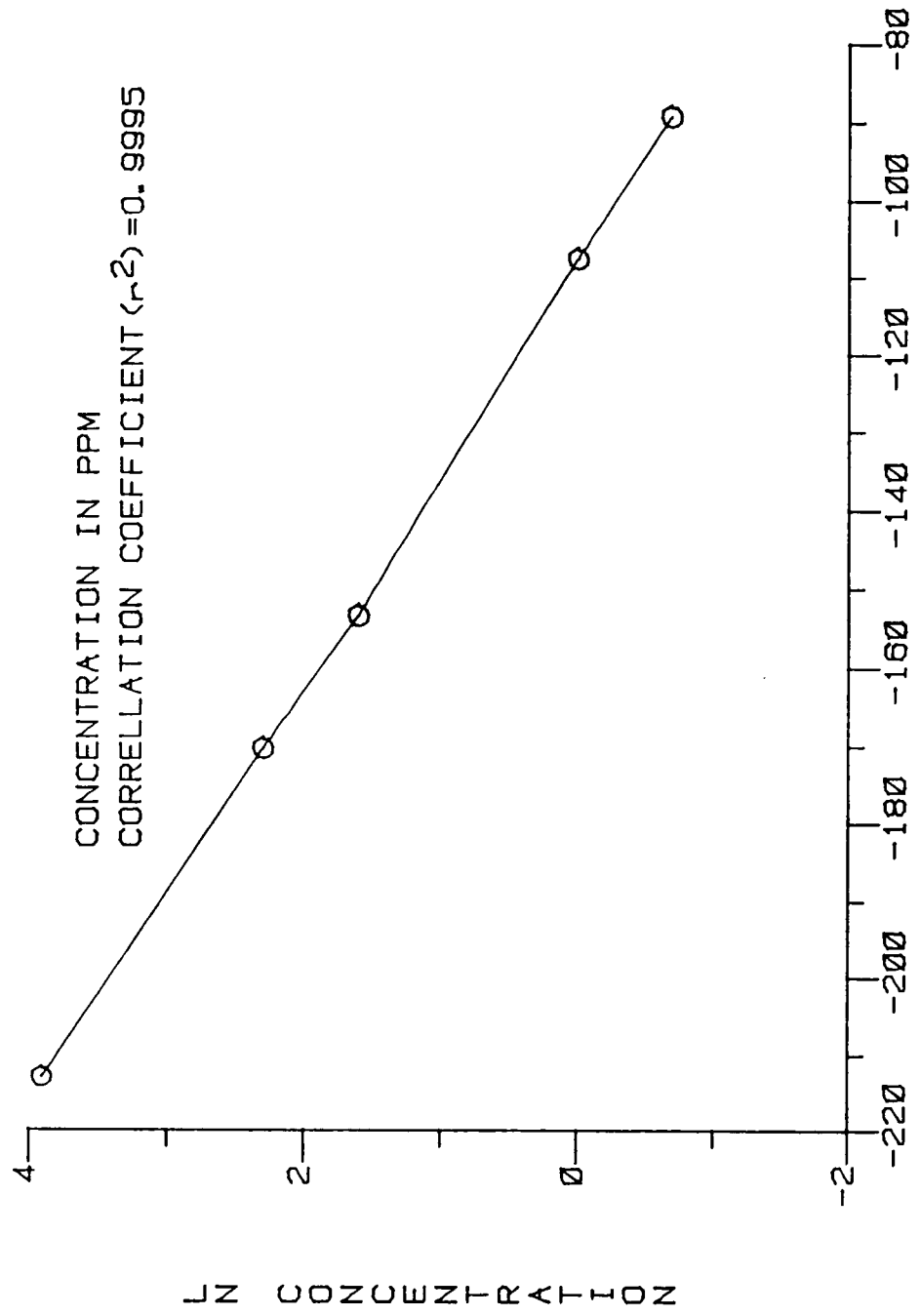

Figure 16. Calibration Curve for the Cyanide Specific Electrode.

3.1.3 Hydrogen Sulfide Analysis. In addition to the previous analyses of the nitrogen species, the hydrogen sulfide (H_2S) concentration in the dry sample gas was monitored at selected times during the tests. Before each "bubble sample" was taken a bag sample was collected which was later analyzed on a Perkin Elmer Model Sigma 2B gas chromatograph. This analysis was done by Bill Baucum and the results are shown in Table 12.

3.2 Determination of Other Constituents in Combustion Gas

Several other species were continuously monitored at the SCI sample location during tests. These included nitrogen oxide (NO) and carbon monoxide (CO). The NO concentration in the dry sample gas was determined by a Thermo-Electron Corporation (TECO) Model 10AR $NO-NO_2-NO_x$ gas analyzer. A Beckman Model 864 Infrared Analyzer was used to determine the CO levels. In addition, there existed the capability to divert the sample gas from the SCI location to a Bendix 9000 Analyzer control which outputs the concentrations of CO, N_2, O_2, H_2S, CO_2, CH_4, and H_2. The results of interest from these analyses were obtained from the test reports and are shown in Tables 13 and 14.

Test 12. Results of Hydrogen Sulfide Analysis.

Sample No.	Test	Time	H_2S Concentration (PPM Dry Gas)
1	LMF3B-2a	8:50 A.M.	1640
2	LMF3B-2b	8:07 A.M.	2170
3	LMF3B2b	9:50 A.M.	2230
4	LMF3B-2b	12:02 P.M.	2480

Table 13. Results of Nitrogen Oxide and Carbon Monoxide Analyses.

Sample No.	Test	Time	NO Concentration (PPM dry gas)	CO Concentration (PPM dry gas)
1	LMF3B-2a	8:50 A.M.	156	64,000
2	LMF3B-2b	8:07 A.M.	150	52,000
3	LMF3B-2b	9:50 A.M.	125	59,000
4	LMF3B-2b	12:02 P.M.	130	54,000

Table 14. Results from On-Line GC for LMF3B-2b.

Time	CO[a]	N_2[a]	O_2[a]	H_2S[a]	Time	CO_2[a]	CH_4[a]	H_2[a]
10:16 A.M.	60,000	608,000	20,000	NA	10:16 A.M	296,000	NA	17,000
11:38 A.M.	39,000	537,000	17,000	NA	11:38 A.M.	249,000	NA	7,000

[a]The concentrations are in PPM dry gas.

NA: Readings not available or inaccurate.

4.0 RESULTS

4.1 Flow Characteristics and Heat Transfer Analysis Through the Sample Probe

The sample probe was modeled as a plug-flow cylindrical reactor with constant surface temperature. The flow through the probe was in the laminar regime and should reach fully developed conditions within the first two centimeters of the sample probe. The Nusselt number for the heat transfer occurring in the probes was determined to be 8.36. This yielded average convective heat transfer coefficients of 17.8 W/m^2K for the RF1 probe and 14.0 W/m^2K for the SCI probe. The gas cooling profiles created for the RF1 sample probe using the PROF code and theoretically calculated showed very good agreement with the experimental cooling profile (Figures 12 and 13, pp. 38 and 39).

4.2 Reaction Kinetics Through the Sample Probe

The theoretical results derived using the PROF and NASA codes were compared with experimental results collected during the LMF3B test series. The combined results are listed in Tables 15 and 16 for tests LMF3B-2a and LMF3B-2b, respectively. The agreement between the experimentally determined and PROF predicted values of N_2 was very good for test LMF3B-2b. For both tests the experimental CO values were less than 50 percent of the PROF predicted value while for test LMF3B-2b the PROF predicted values of CO_2 was 13 percent less than the experimental value. Also, the experimental H_2 values were only about half as much as the PROF predicted values. These discrepancies could in part be due to the water-gas-shift reaction:

Table 15. Comparison of Experimental and Theoretical Concentrations for Test LMF3B-2a.

Species	Experimental (PPM dry gas)	PROF (PPM)	PROF (PPM dry gas)
CO	64,000[a]	102,030	119,960
NO	156[a]	83	96
NH_3	13[b]	18	21
H_2S	1,640[c]	257	302

[a]Determined from test report.

[b]Determined using ion selective electrode method.

[c]Determined using a gas chromatograph.

Table 16. Comparison of Experimental and Theoretical Concentrations for Test LMF3B-2b.

Species	Experimental (PPM dry gas)	PROF (PPM)	PROF (PPM dry gas)
CO	55,000[a]	106,020	122,782
CO_2	296,000[c]	227,740	257,959
NO	135[a]	65	75
NH_3	27[b]	17	20
N_2	608,000[c]	506,340	595,323
O_2	20,000[c]	0.02	0.02
H_2	17,000[c]	27,761	32,640
H_2S	2,290[c]	261	302

[a]Determined from test report.

[b]Determined using ion selective electrode method.

[c]Determined using a gas chromatograph.

$$CO + H_2O \rightleftarrows CO_2 + H_2 \qquad (18)$$

The experimental O_2 value for test LMF3B-2b was much higher than the value predicted by PROF. This could be caused by air leaks along the flow train prior to the secondary combustor. The experimental and PROF predicted values for H_2S did not agree very well. The PROF predicted value for H_2S was five times less than the experimental value for test LMF3B-2a and about eight times less for test LMF3B-2b. This is consistent with the fact that PROF predicted unusually high values of SO_2, which was noted earlier. The values of NH_3 and NO showed results which were consistent with trends noticed in the theoretical analysis. The experimental and PROF predicted values for NH_3 were fairly close considering the low concentrations which had to be detected. The NO concentration predicted with PROF was about 40 percent less than the experimental value. This is fairly consistent with the 30 percent drop in concentration predicted by PROF in the theoretical analysis section. Overall, the nitrogen species showed good agreement between the experimental and PROF predicted values, while some discrepancy was noticed for the carbon and sulfur species.

5.0 CONCLUSIONS AND RECOMMENDATIONS

The following conclusions can be made from analysis of the theoretical calculations and data collected from the LMF3B test series:

1) The thermal characteristics of the gas in the sample probe can be modeled reliably with the PROF code.
2) Most of the reactions occur in the sample probe within the first 20 centimeters where greater than 80 percent of the cooling also takes place.
3) The PROF code modeled the nitrogen species reactions well and established that NO decomposes by about 30 percent through the sample probe at the SCI location while a large increase in the NH_3 concentration is detected. The decomposition of NO predicted by PROF at the RF1 sample location was greater than 80 percent.
4) The flow rate of the gas does not effect the extent of the reactions which occur through the sample probes, only the time and distance into the probe over which the reactions occur.
5) The solids should not affect the reactions in the sample probe because they do not begin to precipitate out until most of the species have reached a steady state concentration.

Much more work remains in understanding the reactions in the gas stream before secondary combustion. A reliable method for the determination of HCN should be developed. Analysis of the gas collected in the bag sample with the gas chromatograph may be possible. Also, the PROF code predicted relatively high levels of N_2O and NOH in the dried sample gas. Analysis for these constituents should be considered.

Further work is needed in the modeling of the sulfur chemical reactions in order to determine what part they plan in the decomposition of NO through the sample probe. In addition, the carbon monoxide reactions should be studied to determine why there is such a large discrepancy between experimental and calculated values.

Finally, the PROF code could be used in analysis of the reactions which occur at other sampling points along the flow train. Determination of the reactions through the sample probes will lead to a more accurate analysis of the actual gas in the flow train.

LIST OF REFERENCES

LIST OF REFERENCES

1. Crawford, Lloyd W., et al., "Nitrogen Oxide Control in a Coal Fired MHD System," E02-0115-013-83, Presented at the 21st Symposium on Engineering Aspects of Magnetohydrodynamics, June 27-29, 1983.

2. Kendall, Robert M., and Kelly, John T., "Premixed One-Dimensional Flame (PROF) Code User's Manual," EPA-600/7-78-172a, August, 1978.

3. Gordon, Sanford, and McBride, Bonnie J., "Computer Program for Calculations of Complex Chemical Equilibrium Compositions, Rocket Performances, Incident and Reflected Shocks, and Chapman-Jouguet Detonations," NASA Lewis Reserch Center, NASA SP-273, 1971.

4. Galanga, Fred L., "A One-dimensional Code to Predict Thermal Behavior of the UTSI MHD Radiant Furnace," DOE/ET/10815-88, March, 1984.

5. Incopera, Frank P., and Dewitt, David P., "Fundamentals of Heat Transfer," John Wiley and Sons, New York, New York, pp. 390, 401-405, 1981.

6. McCabe, Warren L., and Smith, Julian C., "Unit Operations of Chemical Engineering," McGraw-Hill, Inc., p. 298, 1976.

7. Hanley, H. J. M., and Ely, James F., "The Viscosity and Thermal Conductivity of Dilute Nitrogen and Oxygen," Journal of Physical and Chemical Reference Data, Volume 2, No. 4, pp. 733-756, 1976.

8. Muzio, L. J., Arand, J. K., and Teveira, D. P., "Gas Phase Decomposition of Nitric Oxide in Combustion Products," EPRI Contract RP 461-1, Sixteenth Symposium (International) on Combustion, p. 199, August 15-20, 1976.

9. Blair, D. W., Wendt, J. O. L., and Bartok, W., "Evolution of Nitrogen and Other Species During Controlled Pyrolysis of Coal," NSF/RANN Grant No. AER 75-03964, Sixteenth Symposium (International) on Combustion, p. 475, August 15-20, 1976.

10. Song, Y. H., Blair, D. W., Siminski, V. J., and Bartok, W., "Conversion of Fixed Nitrogen to N_2 in Rich Combustion," Eighteenth Symposium (International) on Combustion," p. 55, August 17-22, 1980.

11. Burkinshaw, Jeffry R., Smoot, L. Douglas, Hedman, Paul O., and Blackman, Angus U., "Analysis of Sulfur and Nitrogen Pollutants in Three-Phase Combustion Effluent Samples," Industrial and Engineering Chemistry Fundamentals, Vol. 22, pp. 292-298, 1983.

APPENDIXES

APPENDIX A

6:29 - GC sampling from AHO
8:46 - GC sampling at AHO. AHO SO_2 and NO_x flow meters turned off to provide adsequate flow to GC.
9:18 - GC sampling at RFl
9:47 - Calibrated RFl CO instrument
9:56 - SCI probe plugged. Also discovered burst airline
9:59 - Switched scale momentarily n the SCI NO instrument
10:02 - Adjusted GC flow to 10 psi
10:21 - Noticed AHO NO_x instrument not showing voltage to DAS. Recorder output found plugged. Plugged in leads.
10:30 - SCO NO_x and SO_2 flow meters turned off to provide adequate flow to GC. GC now sampling at SCO.
10:55 - GC sampling at AHO. SO_2 and NO_x flow meters turned off at AHO to provide adequate flow to GC. SCO NO_x and SO_x flow meters turned on again.
11:30 - Rodded out DFO
11:32 - AHO SO_2 and NO_x flow meters on again. GC put in idle mode.
12:09-12:11 - Grab sample taken from DFO
12:12-12:15 - Grab sample taken from RFl.
12:16-12:20 - Grab sample taken from SCI.
12:21-12:25 - Grab sample taken from SCO.
12:38 - DFO flow meter turned off to provide adequate flow to GC
1:24 - RFl and SCI CO instruments checked with 10% cal gas. Both were within 0.5%
1:28 - RFl and SCI pumps on pulling samples from respective locations.
1:30 - All sample pumps off except AHO. CO_2, O_2 and CO only being sampled of AHO.

Note: DFl: First Diffuser Probe
DFO: Diffuser Outlet
SCO: Secondary Combustor Outlet
AHO: Air Heater Outlet

Figure A-1. Gas Sampling Notes from Test LMF3B-1.

6:59 - All analyzers sampling from respective probe positions
8:48 - Discovered low flow at RF1 NO. Turned flow meter up. No problem.
8:48 - Took bag sample from SCI for lab GC analysis
8:50 - Dennis Knisley "bubbled" sample from SCI for NH_3 and HCN.
9:09 - Checked pacillaries and calibration on SCI NO instrument
9:20 - On-line GC sample from DFO.
9:30 - Changed SCI NO instrument to 0-1000 ppm
9:36 - On-line GC sampling at RF1.
10:08 - Noted high NO_x at SCI, SCO and AHO. Also high CO at SCI, SCO and AHO, and low CO_2 at AHO.
10:15 - Checking for H_2O accumulation in sample gas condensers when called inside.

Failed to record times, but used instrument air as "lance" to clear DF1 probe blockage.

Note: DF1: First Diffuser Probe
DFO: Diffuser Outlet
SCO: Secondary Combustor Outlet
AHO: Air Heater Outlet

Figure A-2. Gas Sampling Notes from Test LMF3B-2b.

5:00 - SCO CO_2 instrument fixed and calibrated. IR source arrived day before
6:43 - GC sampling at AHO
7:54 - GC switched from AHO to SCO
7:58 - SCO NO_x and SO_2 turned off to receive adequate flow to GC
8:04 - DF1 sample started
8:06 - GC in idle mode
8:07 - SC1 NO and CO flow meters turned off. SCI bag sample and "bubbled" sample for NH_3 and HCN taken
8:51 - DF1 blown out
8:55 - SCO, CO AND CO_2 flow meters turned off
8:56 - GC sampling at SCO
8:57 - DFO dductor cleaned
8:59 - DF1 line blown out
9:14 - GC sampling at AHO. SCO CO_2 and CO flow meters on again
9:15 - AHO NO_x, CO and CO_2 flow meters off
9:18 - DF1 probe and line blown out
9:30 - DFO rodded out
9:37 - DF1 probe and line blown out
9:47 - GC not sampling. AHO NO_x CO and CO_2 flow meters turned on again.
9:50 - SCI bag sample taken and SCI "bubbler" sample for HCN and NH_3 taken
9:51 - SCI NO and CO flow meters off
10:10 - DF1 water pot emptied
10:12 - AHO water pot checked
10:13 - RF1 water pot checked
10:14 - SCO and DFO water pots checked
10:16 - GC sampling at SCI. SCI NO and CO flow meters turned off
10:55 - GC switched from SCI to SCO
11:18 - SCI NO and CO flow meters turned on again
11:38 - GC switched from SCO to SCI
11:40 - SCI bag sample taken
11:42 - SCO NO_x and SO_2 flow meters turned on again
11:52 - SCI NO and CO flows turned on
12:02 - SC1 NO flow meter turned off and sample "bubbled" for HCN and NH_3.
12:47 - GC sampling from AHO. AHO CO_2, CO and NO_x flow meters off
12:51 - SC1 NO and CO flow meters restored
1:00 - RF1 probe plugged. (Probe with 16 T/C's, could not rod out). All flow to NO and CO off

Figure A-3. Gas Sampling Notes from Test LMF3B-2b.

1:18 - GC sampling at SCO. SCO SO_2, NO_x, CO, AND CO_2 flow off. AHO NO_x and SO_2 on again.
1:21 - SCI sampling pump off in order to check calibration of NO instrument. Used 340 ppm standard. Machine read 345 ppm. Turned flows on again
1:32 - AHO SO_2 flow meter low. Turned flow up and SO_2 showed approximately 100 ppm higher
1:35 - GC switched from SCO to SCl. SCO NO_x, SO_2, and CO_2 and CO flow meters on. SCl NO and CO flow meters turned off
1:55 - GC switched to idle mode
2:00 - SCl NO and CO flow meters on and GC switched to DFO
2:27 - DFO sampling pump off. SCl sampling pump off.

SCI - NO flow meter off due to inadequate flow. CO at SCl left operating. Adequate flow for it to operate.

Note: DFl: First Diffuser Probe
DFO: Diffuser Outlet
SCO: Secondary Combustor Outlet
AHO: Air Heater Outlet

Figure A-3 (Continued)

APPENDIX B

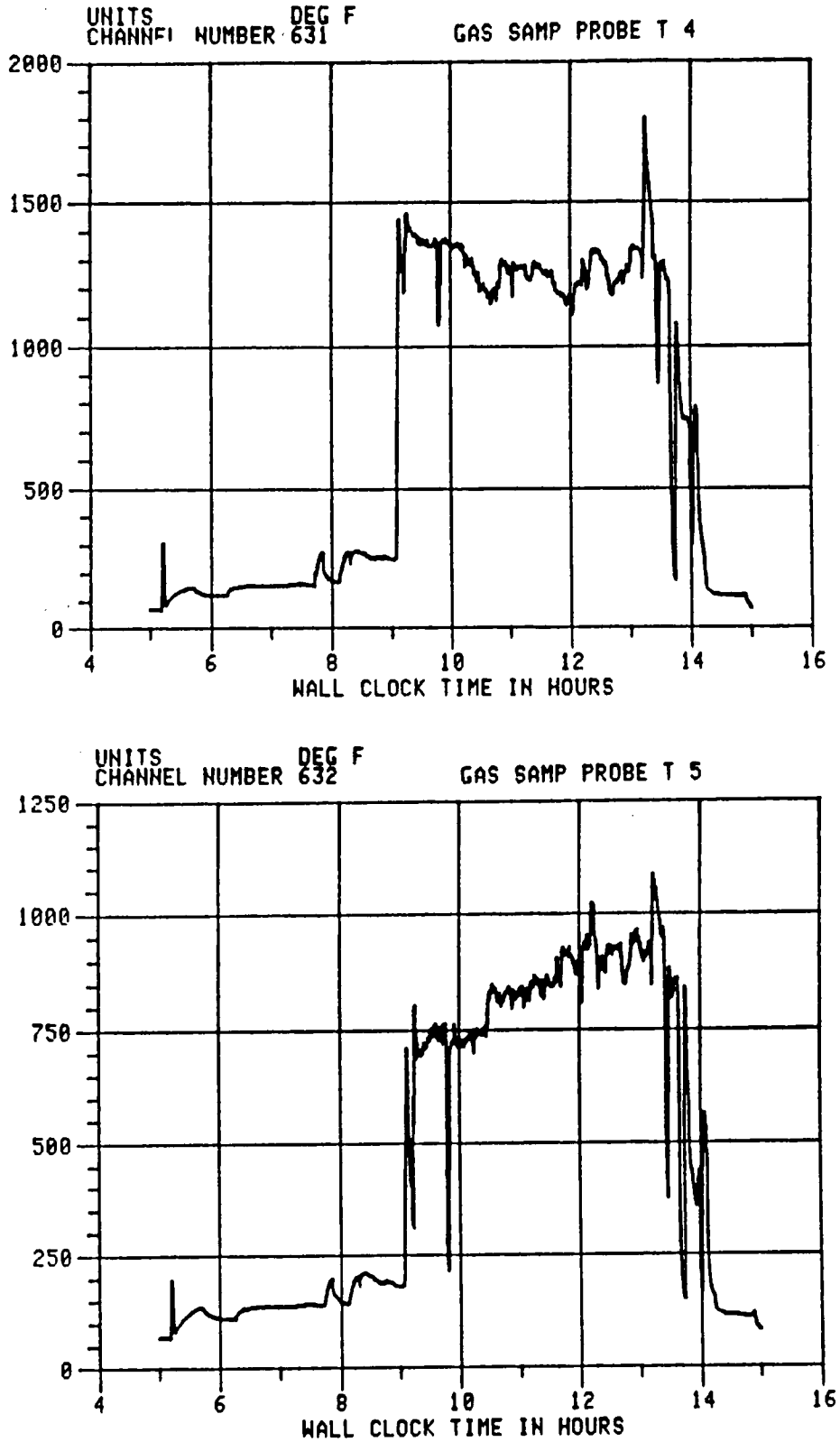

Figure B-1. Gas Temperature Data Collected at the RF1 Sample Location during Test LMF3B-1.

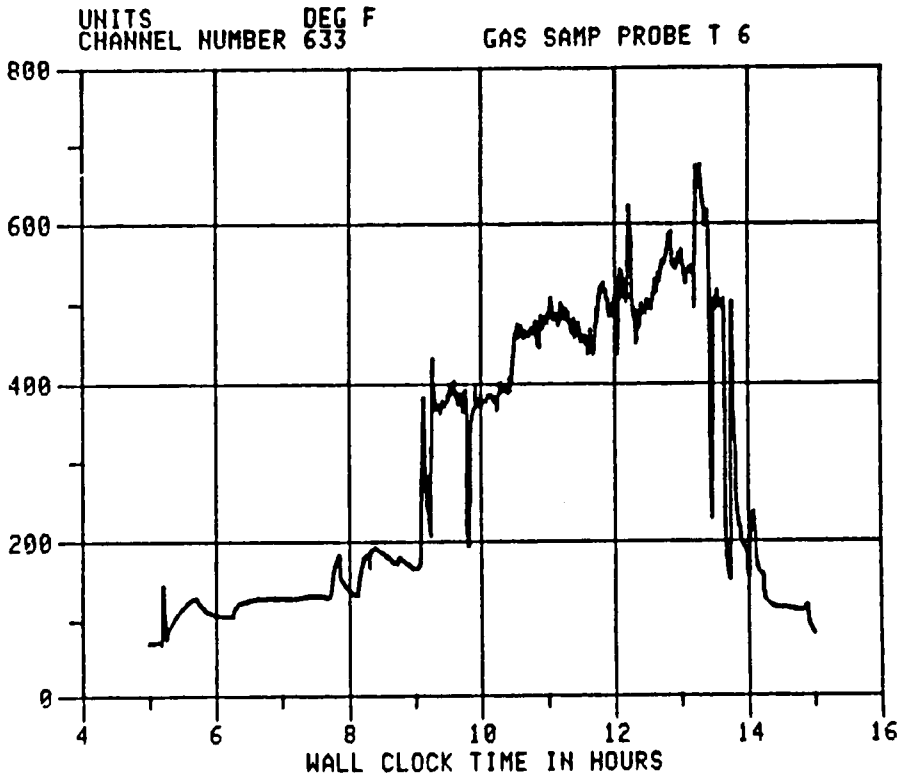

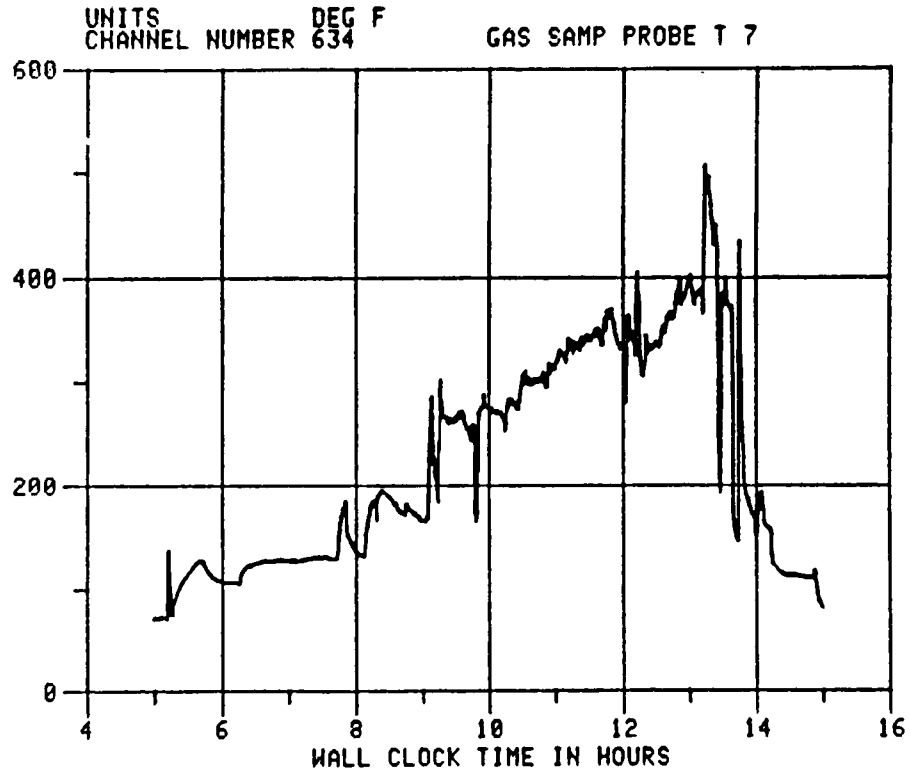

Figure B-1 (Continued)

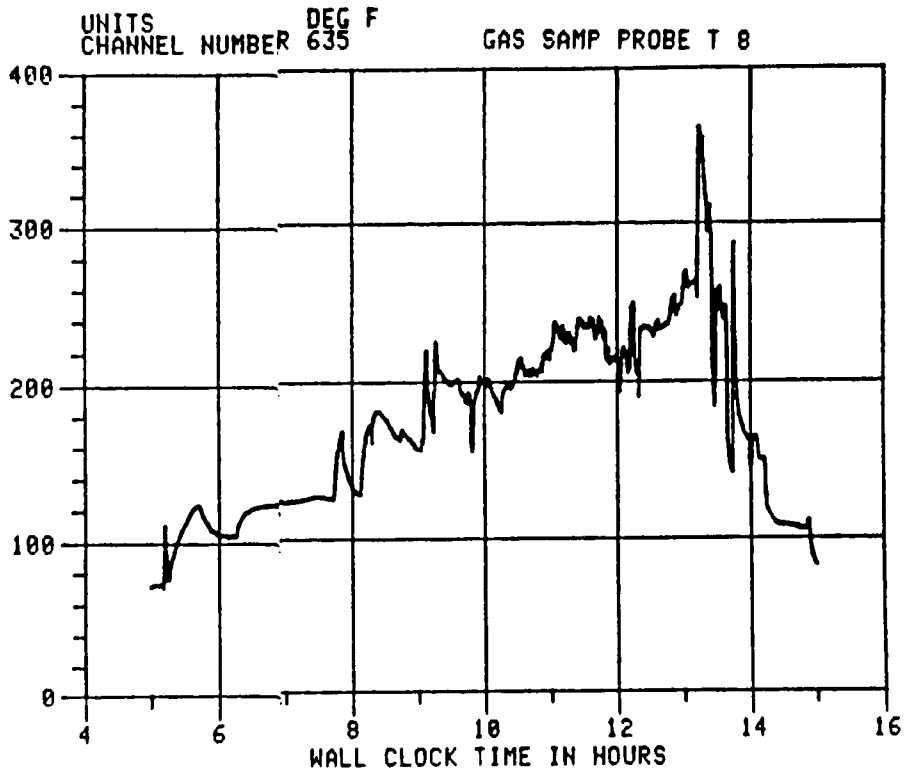

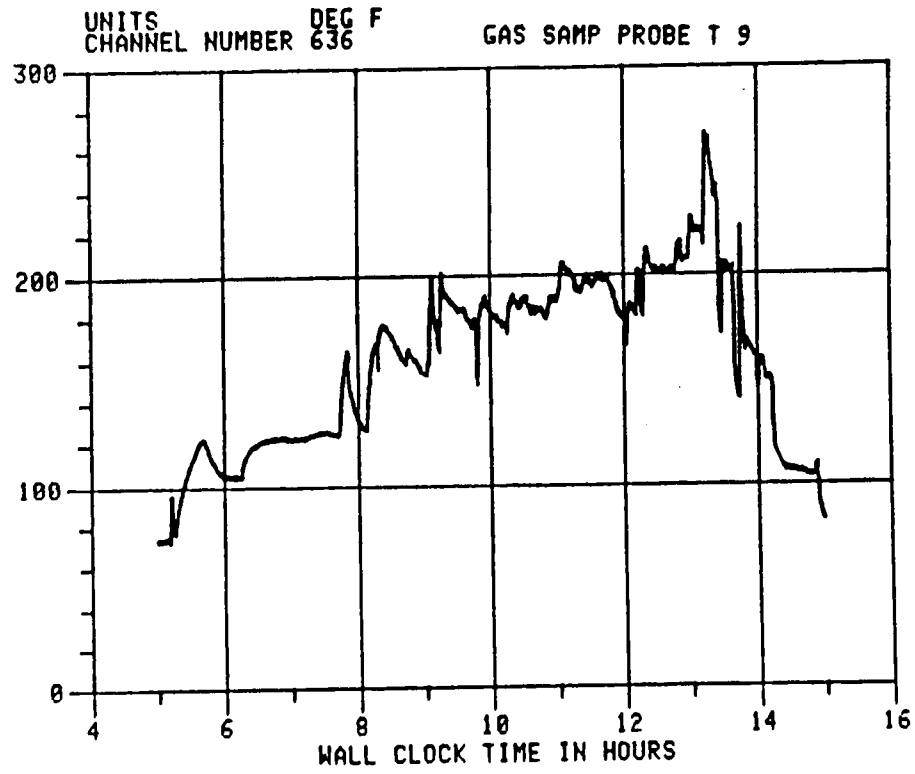

Figure B-1 (Continued)

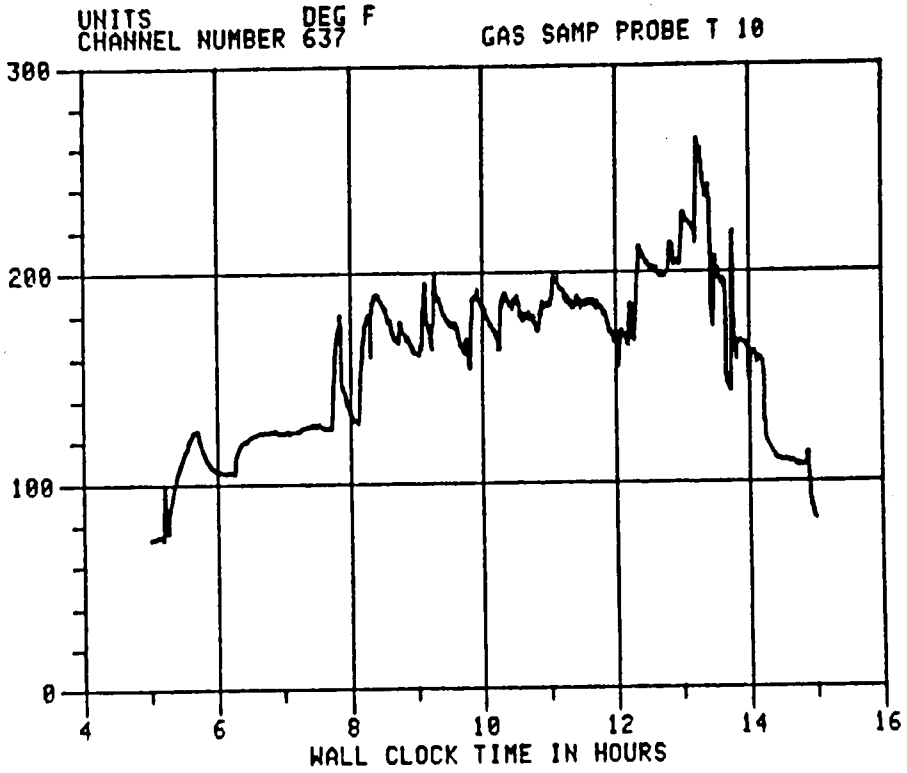

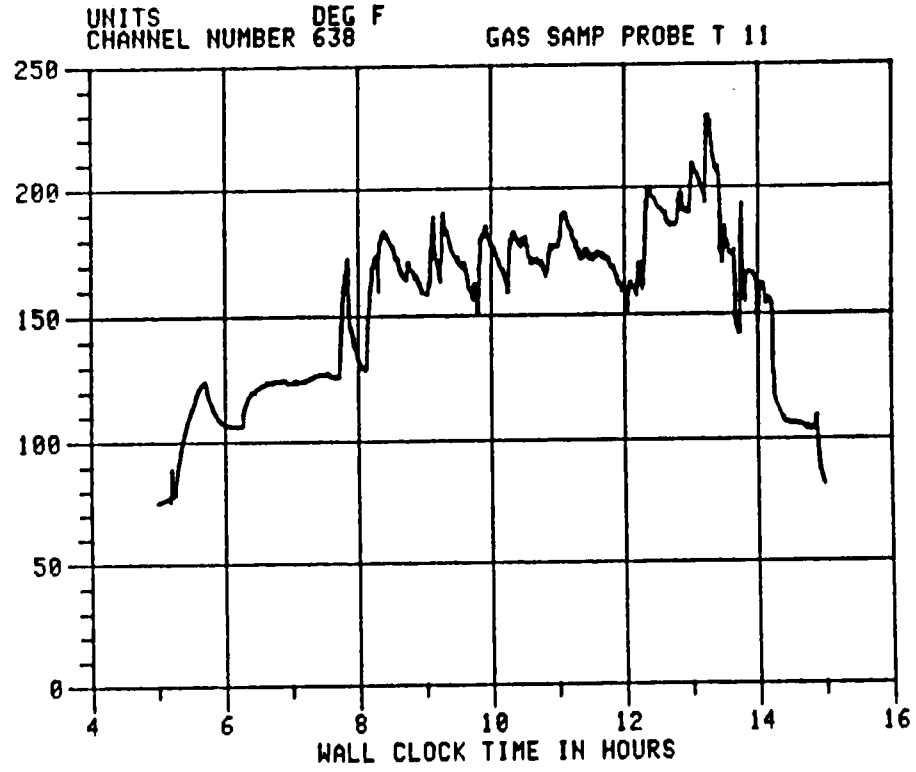

Figure B-1 (Continued)

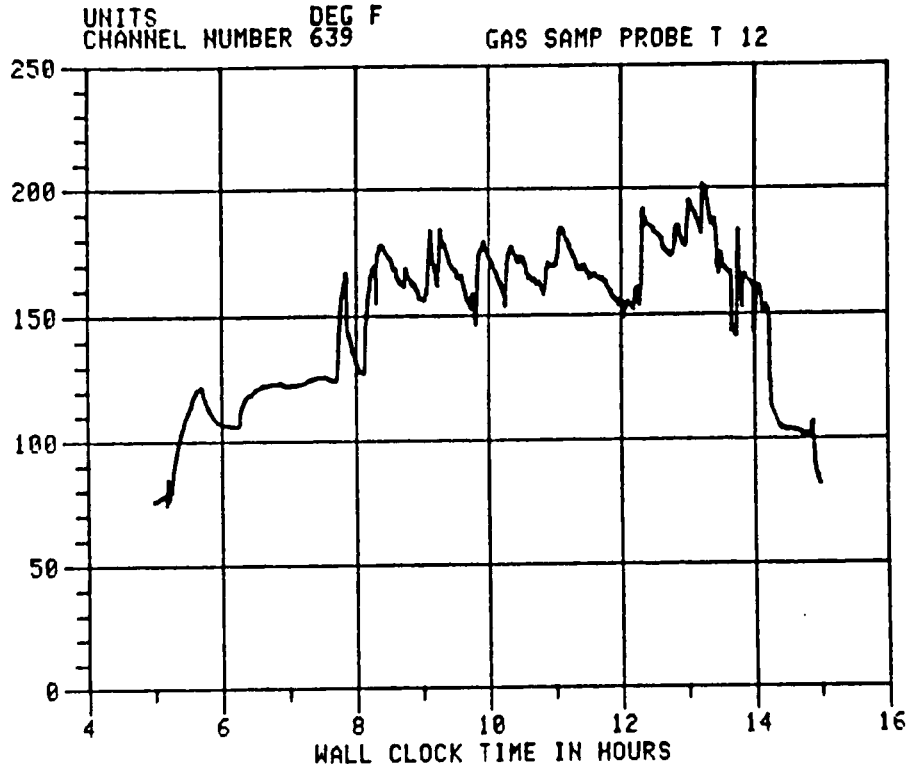

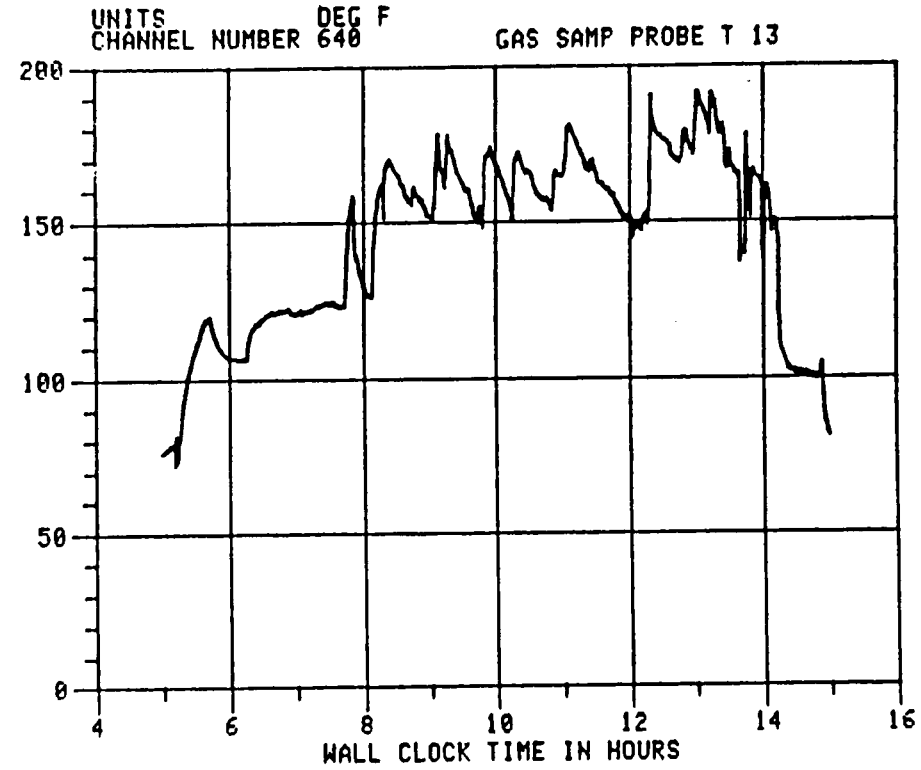

Figure B-1 (Continued)

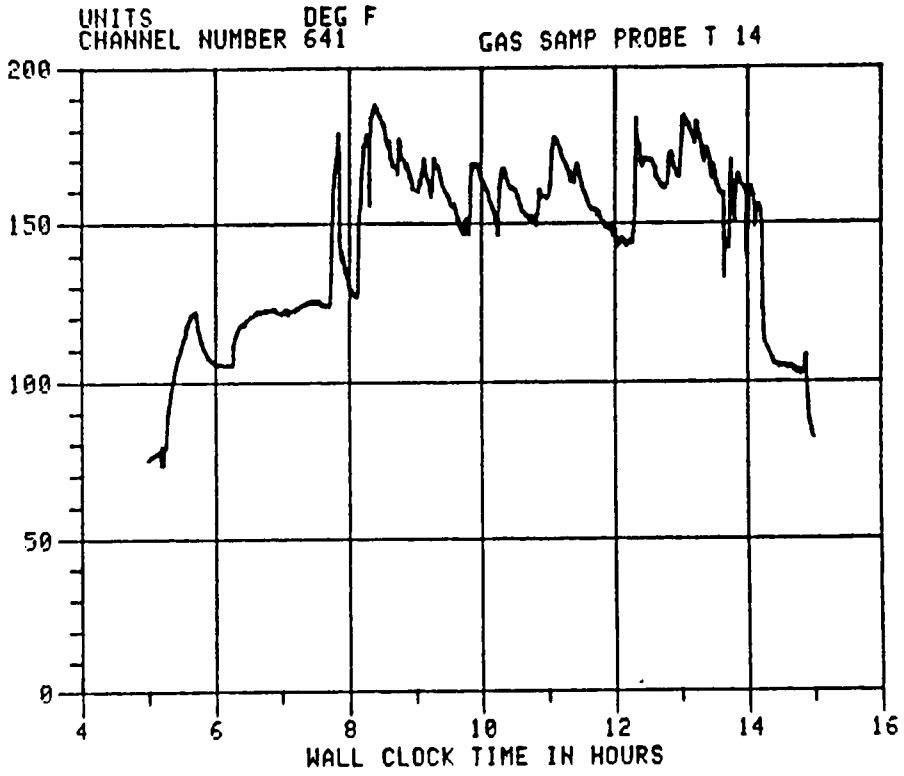

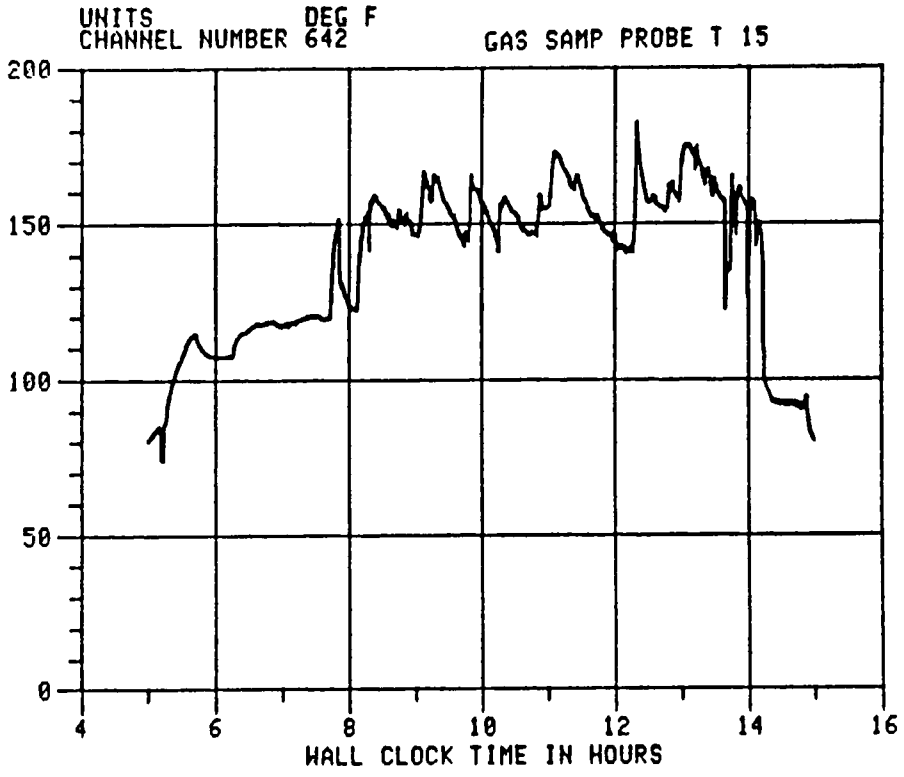

Figure B-1 (Continued)

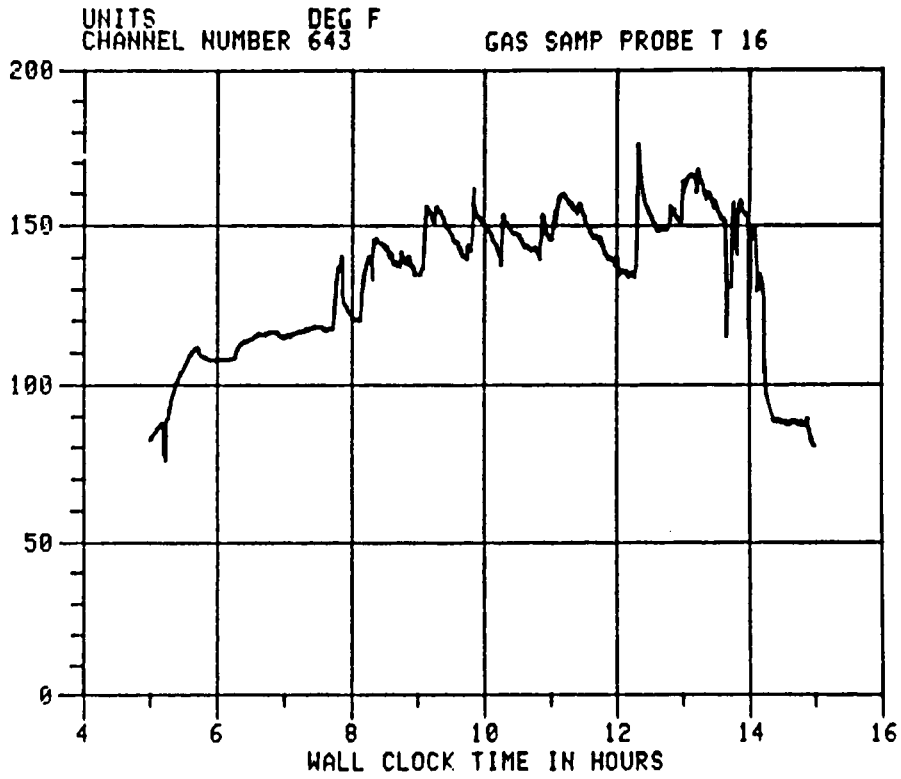

Figure B-1 (Continued)

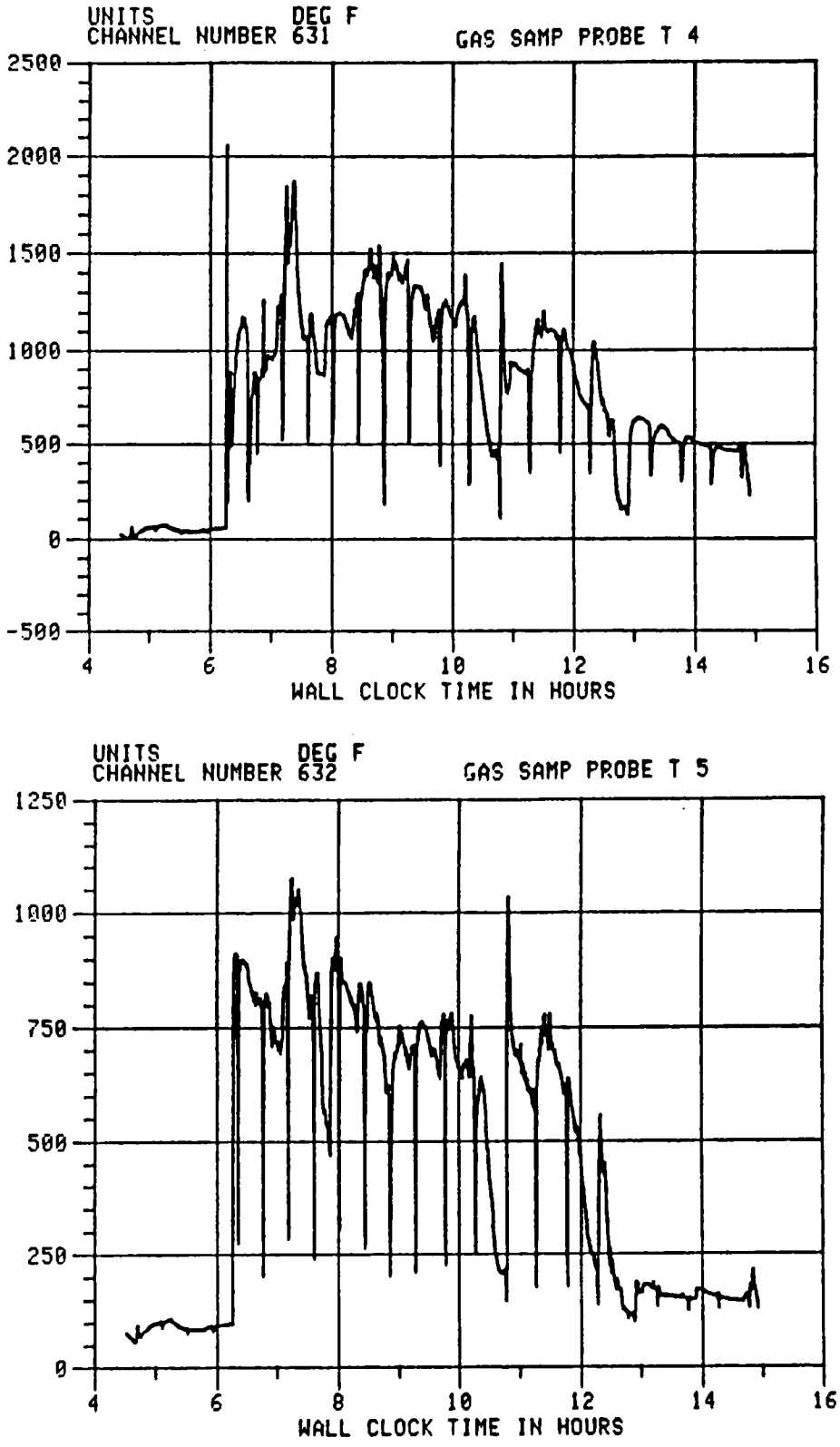

Figure B-2. Gas Temperature Data Collected at the RF1 Sample Location During Test LMF3B-2b.

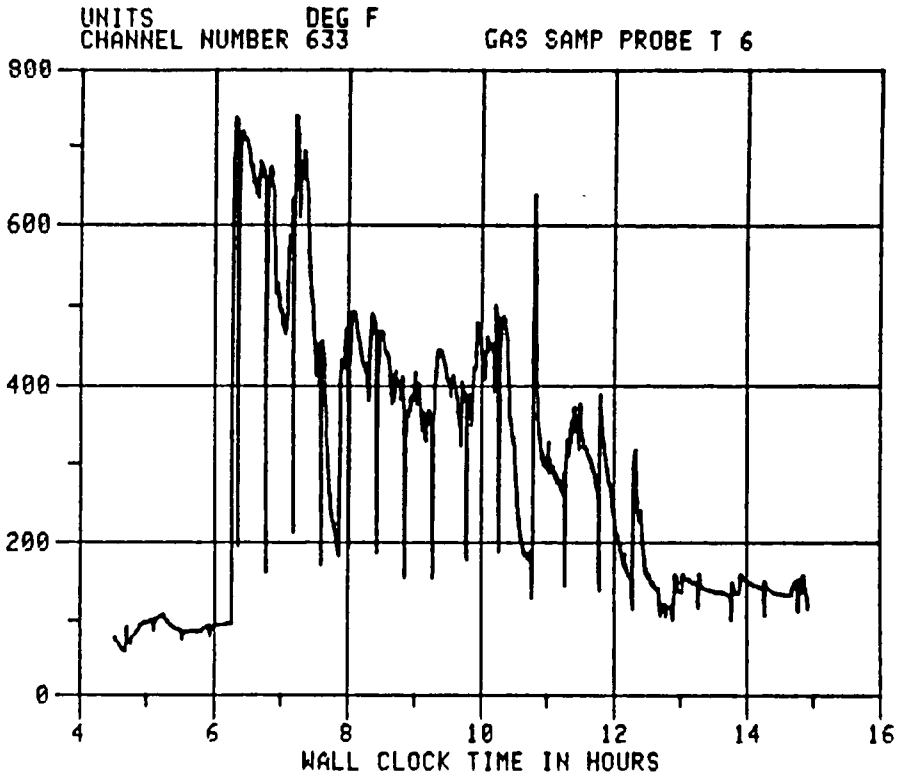

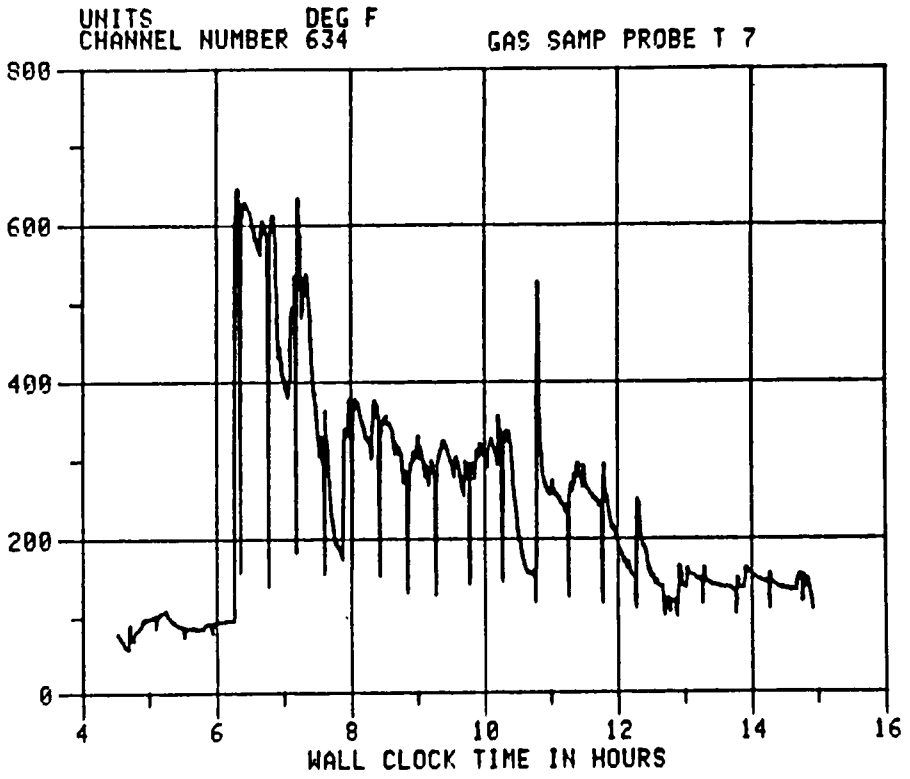

Figure B-2 (Continued)

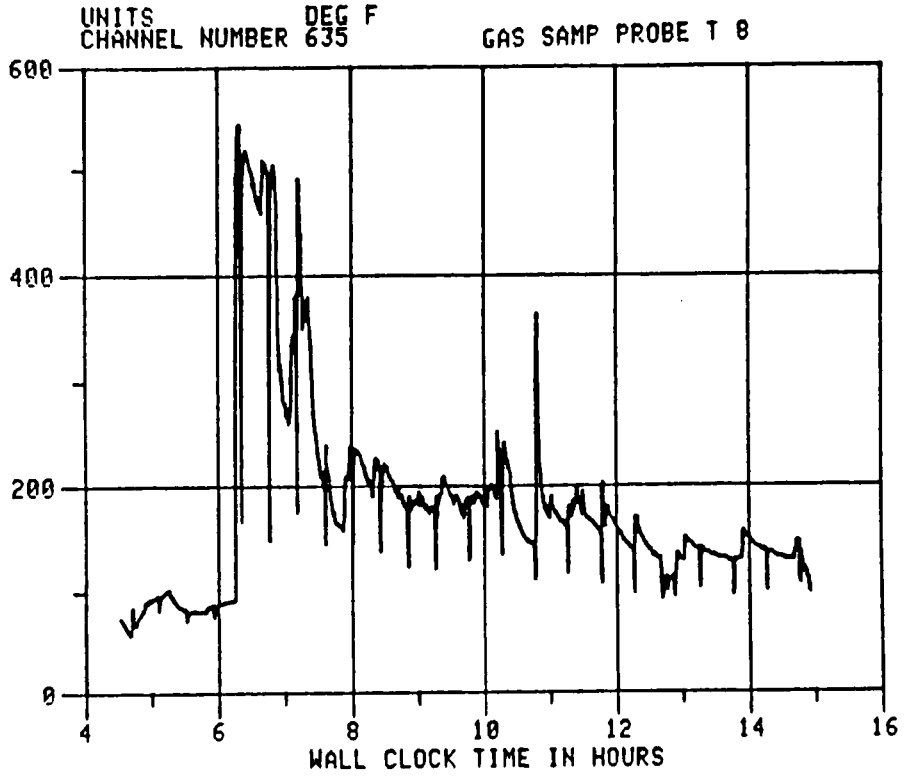

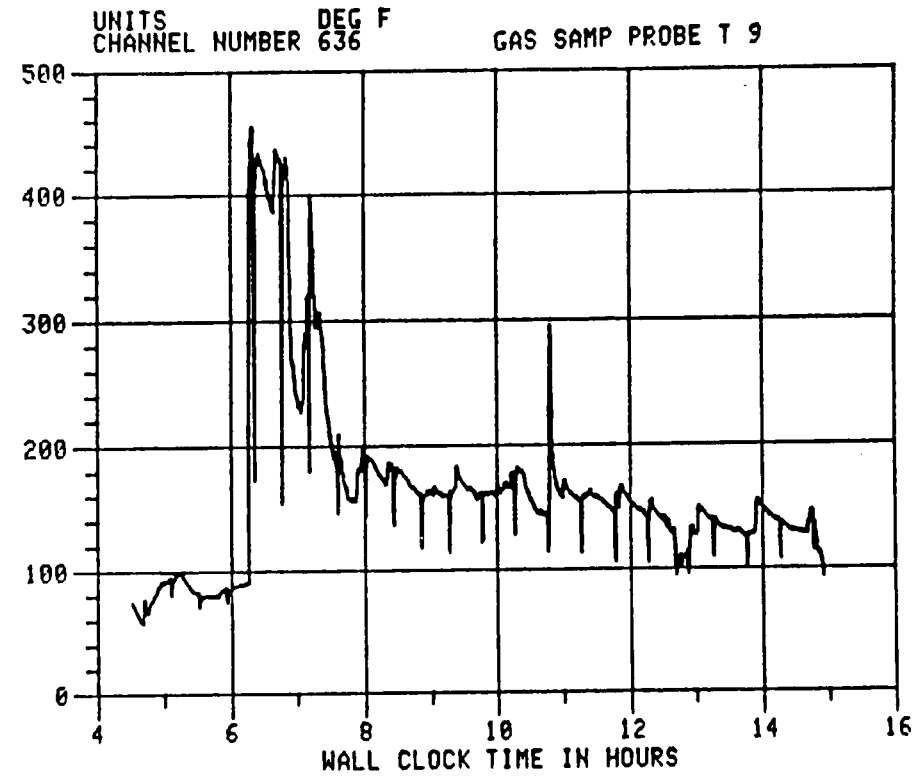

Figure B-2 (Continued)

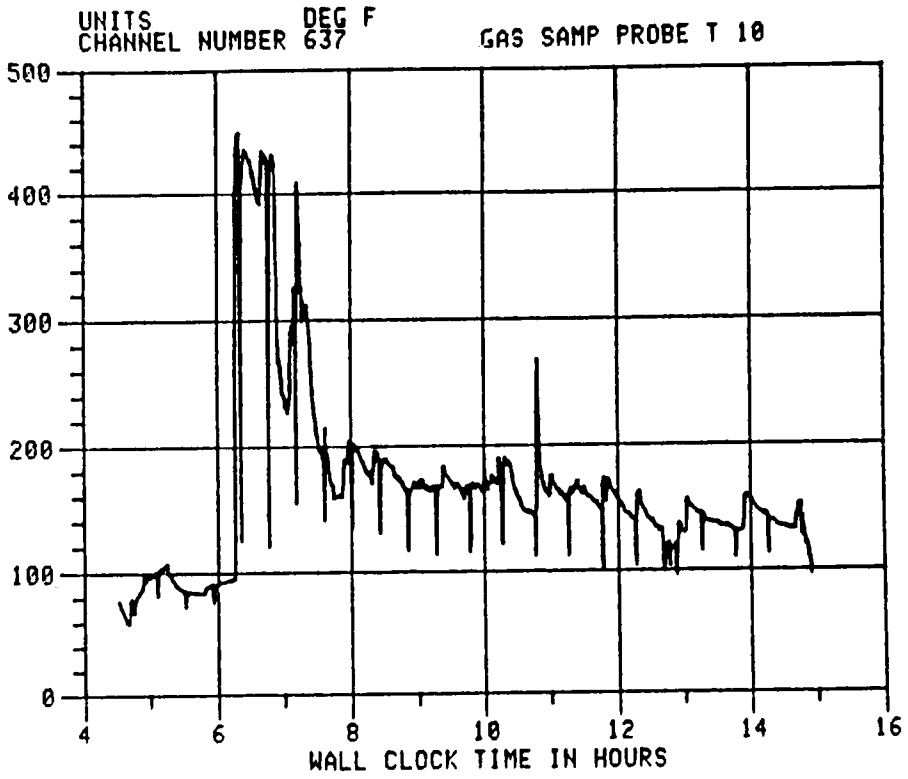

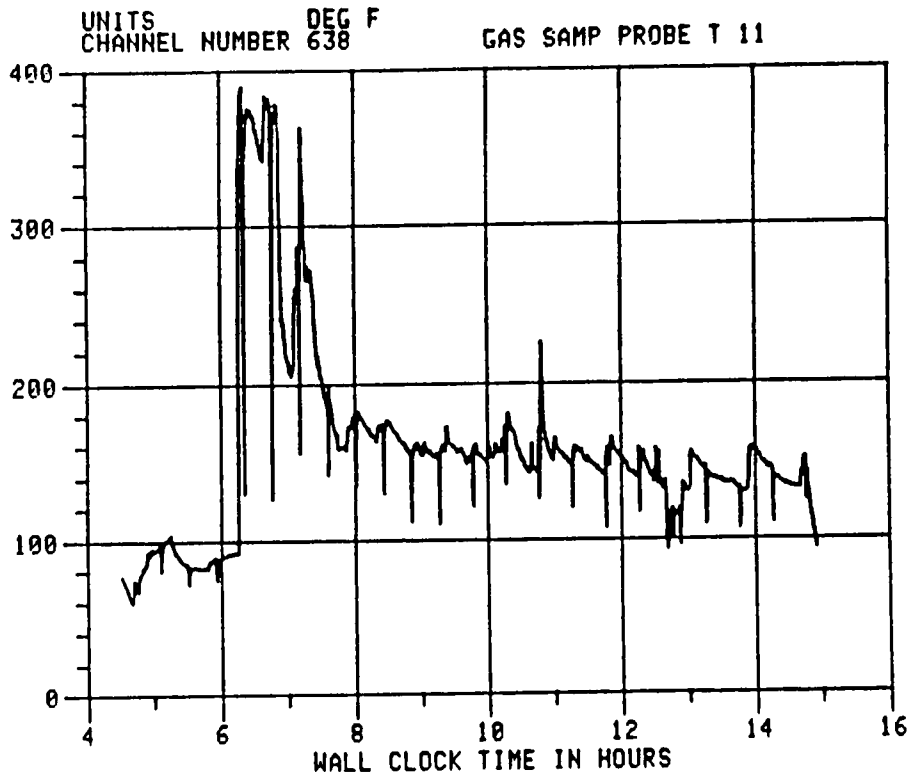

Figure B-2 (Continued)

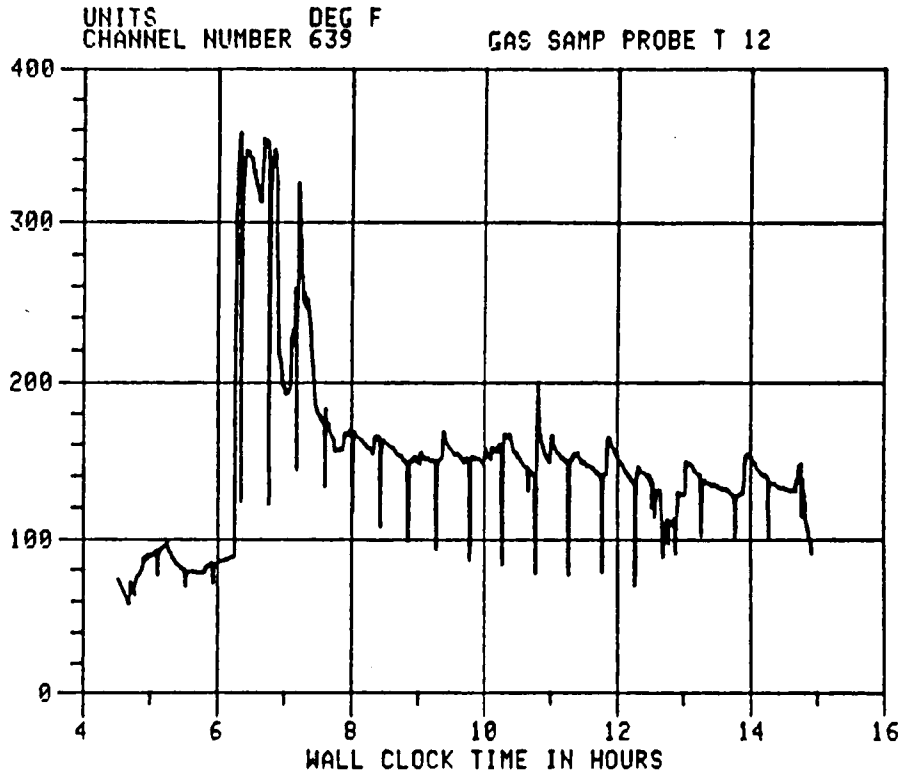

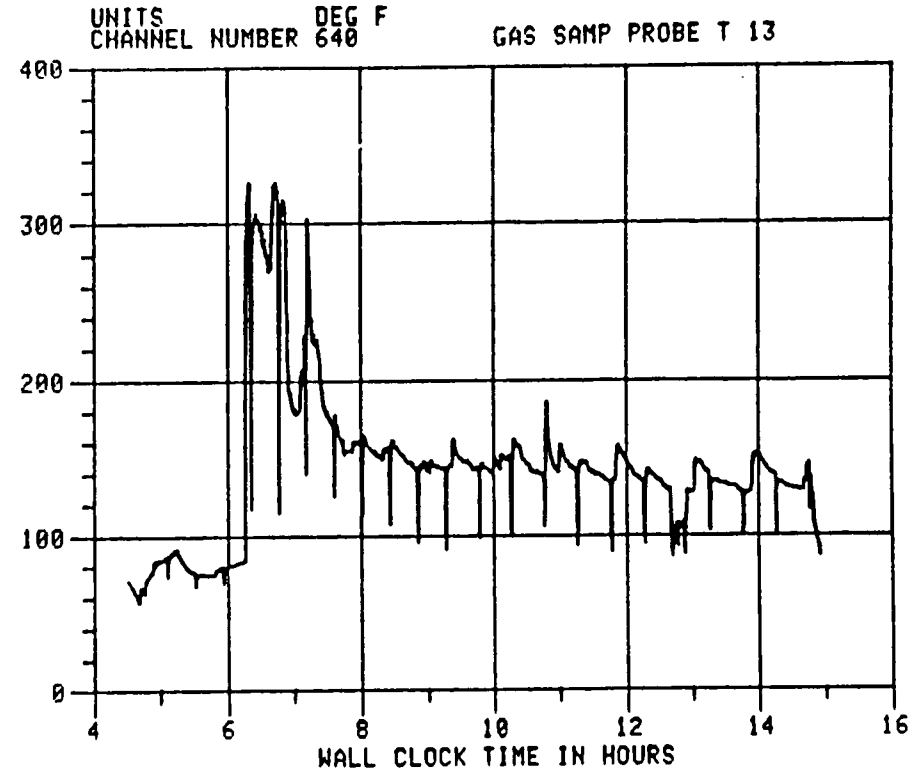

Figure B-2 (Continued)

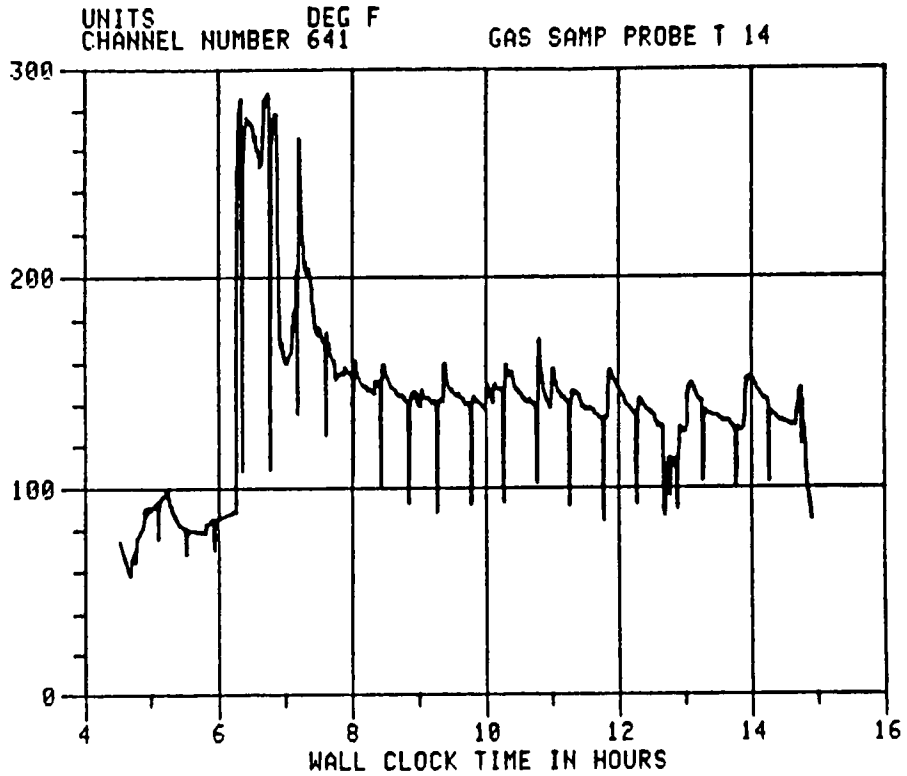

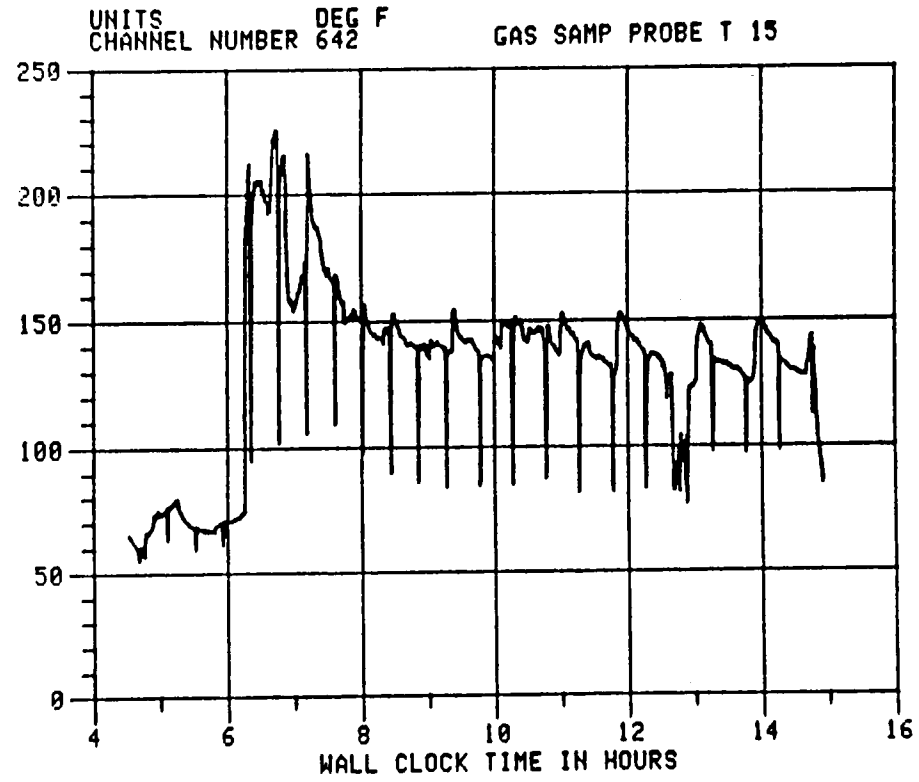

Figure B-2 (Continued)

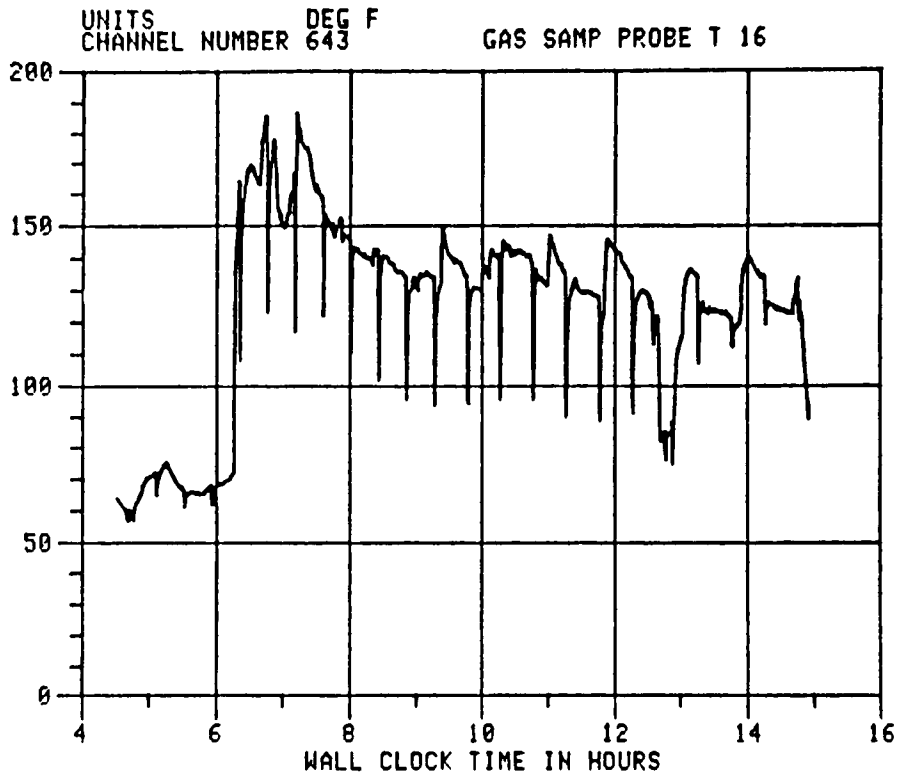

Figure B-2 (Continued)

APPENDIX C

```
      OPEN (UNIT=1,NAME='RENTHAL3.DAT',TYPE='OLD')
      WRITE(1,51Ø)
  51Ø FORMAT(5X,'X(M)',5X,'TX',8X,'TXDX',7X,'HX',6X,'HXDX')
C ENTER INTIAL TEMPERATURE AND CORRESPONDING ENTHALPY
      TX=2Ø5Ø.
      HX=-383.37
   5Ø TXDX=TX-25.Ø
C CALCULATE THE AVERAGE TEMPERATURE
      TAVG=(TX+TXDX)/2
C CALCULATE THE THERMAL CONDUCTIVITY
  1ØØ CALL COND (TAVG,TC)
C CALCULATE DELTA H
      DH=(TC)*(TAVG-335.Ø)*Ø.9Ø7ØØ75
C CALCULATE H AT X+DELTA X
      HXDX=HX-DH
C FIND THE TEMPERATURE PREDICTED BY NASA-SP273 AT HXDX
      TEMP=TXDX
      CALL ENTHALPY (HXDX,TXDX)
      IF (ABS(TXDX-TEMP).LT.Ø.1) GO TO 2ØØ
      TAVG=(TX+TXDX)/2
      GO TO 1ØØ

  2ØØ X=X+Ø.Ø1
      WRITE(1,5ØØ)X,TX,TXDX,HX,HXDX
  5ØØ FORMAT(1X,F8.3,2X,F8.2,2X,F8.2,2X,F8.2,2X,F8.2)

      IF (TXDX .LT. 336.Ø) GO TO 3ØØ

      TX=TXDX
      HX=HXDX
      GO TO 5Ø
  3ØØ STOP
      END

C THIS SUBROUTINE CALCULATES THE THERMAL CONDUCTIVITY OF THE GAS
C AT A GIVEN TEMPERATURE FROM DATA GENERATED BY NASA
      SUBROUTINE COND (TAVG,TC)
      IF (TAVG .LT. 7ØØ.Ø) GO TO 55
      IF (TAVG .GT. 7ØØ.Ø .OR. TAVG .EQ. 7ØØ.Ø .AND. TAVG .LT.
     $13ØØ.Ø .OR. TAVG .EQ. 13ØØ.Ø) GO TO 65
      TC=Ø.Ø239542+4.6Ø642E-5*TAVG
      GO TO 75
   65 TC=Ø.Ø122945+5.49956E-5*TAVG
      GO TO 75
   55 TC=Ø.ØØ75Ø9+6.151E-5*TAVG
   75 RETURN
      END

C THIS SUBROUTINE CALCULATES THE ENTHALPY OF THE GAS AT A GIVEN
C TEMPERATURE FROM DATA GENERATED BY NASA
      SUBROUTINE ENTHALPY (HXDX,TXDX)
      IF (HXDX .LT. -925.7 .OR. HXDX .EQ. -925.7) GO TO 57
      IF (HXDX .LT. -818.715 .OR. HXDX .EQ. -818.715 .AND. HXDX
     $.GT. -925.7) GO TO 67
      IF (HXDX .LT. -546.859 .OR. HXDX .EQ. -546.859 .AND. HXDX
     $.GT. -818.715) GO TO 68
      TXDX=(HXDX+1128.14)/Ø.3633ØØ4
      GO TO 77
   67 TXDX=(HXDX+1225.11)/Ø.4926
      GO TO 77
   68 TXDX=(HXDX+1118.36)/Ø.3562541
      GO TO 77
   57 TXDX=(HXDX+1Ø96.7)/Ø.285
   77 RETURN
      END
```

Figure C-1. Program Utilizing Equation 14 to Produce a Temperature Profile for the RF1 Sample Probe: Test LMF3B-1.

```
      OPEN (UNIT=1,NAME='RENTHALB.DAT',TYPE='OLD')
      WRITE (1,51Ø)
  51Ø FORMAT(5X,'X(M)',5X,'TX',8X,'TXDX',7X,'HX',6X,'HXDX')
C ENTER INTIAL TEMPERATURE AND CORRESPONDING ENTHALPY
      TX=2235.Ø
      HX=-433.58
   5Ø TXDX=TX-25.Ø
C CALCULATE THE AVERAGE TEMPERATURE
      TAVG=(TX+TXDX)/2
C CALCULATE THE THERMAL CONDUCTIVITY
  1ØØ CALL COND(TAVG,TC)
C CALCULATE DELTA H
      DH=(TC)*(TAVG-335.Ø)*Ø.9Ø7ØØ75
C CALCULATE H AT X+DELTA X
      HXDX=HX-DH
C FIND THE TEMPERATURE PREDICTED BY NASA-SP273 AT HXDX
      TEMP=TXDX
      CALL ENTHALPY(HXDX,TXDX)
      IF (ABS(TXDX-TEMP).LT.Ø.1) GO TO 2ØØ
      TAVG=(TX+TXDX)/2
      GO TO 1ØØ

  2ØØ X=X+Ø.Ø1
      WRITE(1,5ØØ)X,TX,TXDX,HX,HXDX
  5ØØ FORMAT(1X,F8.3,2X,F8.2,2X,F8.2,2X,F8.2,2X,F8.2)

      IF (TXDX .LT. 336.Ø) GO TO 3ØØ

      TX=TXDX
      HX=HXDX
      GO TO 5Ø

  3ØØ STOP
      END

C THIS SUBROUTINE CALCULATES THE THERMAL CONDUCTIVITY OF THE GAS
C AT A GIVEN TEMPERATURE FROM DATA GENERATED BY NASA
      SUBROUTINE COND(TAVG,TC)
      IF (TAVG .LT. 69Ø.Ø) GO TO 55
      IF (TAVG .GT. 69Ø.Ø .OR. TAVG .EQ. 69Ø.Ø .AND. TAVG .LT.
     $13ØØ.Ø .OR. TAVG .EQ. 13ØØ.Ø) GO TO 65
      TC=Ø.Ø239542+4.6Ø642E-5*TAVG
      GO TO 75
   65 TC=Ø.Ø122945+5.49956E-5*TAVG
      GO TO 75
   55 TC=Ø.ØØ75Ø9+6.151E-5*TAVG
   75 RETURN
      END

C THIS SUBROUTINE CALCULATES THE ENTHALPY OF THE GAS AT A GIVEN
C TEMPERATURE FROM DATA GENERATED BY NASA
      SUBROUTINE ENTHALPY(HXDX,TXDX)
      IF (HXDX .LT. -1Ø93.754 .OR. HXDX .EQ. -1Ø93.754) GO TO 57
      IF (HXDX .LT. -954.8Ø6 .OR. HXDX .EQ. -954.8Ø6 .AND. HXDX
     $.GT. -1Ø93.754) GO TO 67
      IF (HXDX .LT. -673.56 .OR. HXDX .EQ. -673.56 .AND. HXDX
     $.GT. -954.8Ø6) GO TO 68
      TXDX=(HXDX+1278.24)/Ø.3779259
      GO TO 77
   68 TXDX=(HXDX+1269.85)/Ø.37Ø64
      GO TO 77
   67 TXDX=(HXDX+1428.7)/Ø.5582432
      GO TO 77
   57 TXDX=(HXDX+1273.5)/Ø.3Ø52
   77 RETURN
      END
```

Figure C-2. Program Utilizing Equation 14 to Produce a Temperature Profile for the RF1 Sample Probe: Test LMF3B-2b.

VITA

Dennis Ray Knisley was born on February 21, 1960 in Jefferson City, Tennessee. He attended primary school in Kingsport, Tennessee, then moved with his family to Columbia, South Carolina where he graduated from Irmo High School in the Spring of 1978. The next five years were spent at The University of Tennessee as an undergraduate and as a co-op student at Tennessee Eastman Company. The author received his Bachelor of Science degree in Chemical Engineering in June of 1983, then accepted a Research Assistantship at The University of Tennessee Space Institute. The past two years have been spent working toward a Master of Science degree at the Space Institute.